Examination of RF Signal Processing for Cavity BPMs

von

Johannes Nadenau

Masterarbeit in Physik

vorgelegt der

Fakultät für Mathematik, Informatik und
Naturwissenschaften der RWTH Aachen

angefertigt im

III. Physikalisches Institut B, RWTH Aachen

bei

Prof. Dr. Jörg Pretz

September 2018

Ich versichere hiermit an Eides Statt, dass ich die vorliegende Masterarbeit selbstständig und ohne unzulässige fremde Hilfe erbracht habe. Ich habe keine anderen als die angegebenen Quellen und Hilfsmittel benutzt. Die Arbeit hat in gleicher oder ähnlicher Form noch keiner Prüfungsbehörde vorgelegen.

Aachen, den 27.09.2018

Johannes Nadenau

Contents

Introduction

Accelerators for charged particles, e.g. electrons, protons, ions, are used for fundamental physics research (high energy physics, HEP), applied science with synchrotron light, medical applications and many other research areas. Beside the fundamental technical components, i.e. an evacuated beam pipe, magnets providing the guide fields, and RF-driven resonators for the accelerating field, all accelerators and beam-lines require some beam instrumentation devices to quantify the characteristics of the beam, e.g. beam intensity, beam orbit, and emittance, as well as some fundamental machine parameters, like the so-called tune.

The measurement of the beam orbit is based on beam position monitors (BPM), which are electromagnetic detectors with appropriate read-out electronics, distributed along the beam-line of the accelerator. While the basic function is the measurement of the beam orbit, based on the transverse displacement of the beam detected at the BPMs, it enables many additional measurement features, e.g. measurement of beam energy, chromaticity as well as fault finding and analysis.

The operation principle of most BPMs is based on the detection of the image charge of the beam. In this thesis cavity BPMs are discussed. They take a different approach. The BPM pickups are resonant RF cavities, where the amplitude of an eigenmode excited by the beam depends on the beam position. Nowadays, only a few linear accelerator based free-electron laser (FEL) light sources, e.g. at DESY/XFEL (Hamburg, Germany) and at SLAC/LCLS (Stanford, USA) use cavity BPMs for routine operation. This type of BPM offers a resolution in the submicrometer regime for a single passage of the bunched beam.

At the European Organization for Nuclear Research (CERN) in Switzerland the construction of a linear electron collider with a center of mass energy of up to 3 TeV is object of several studies. The project is called Compact Linear Collider (CLIC). To achieve an acceleration gradient of 100 MV/m a two-beam concept is proposed, where the so called drive beam is used to accelerate the main beam.

The presented BPMs are planed for the main beam line of CLIC. The BPM pickups are designed to provide resolution better than 50 nm. A test setup with three of these CLIC cavity BPMs is installed at the CERN Linear Electron Accelerator for Research (CLEAR). Due to the availability of three BPMs the resolution of these BPMs can be obtained by comparing the position determined by one cavity with the ballistic trajectory defined by the two other BPMs.

High resolution BPMs, which are able to determine the position of single bunches, could also be used to determine single particle properties. A particular interesting – and challenging – application is related to the measurement of the electron dipole moment (EDM). Here, one idea is to fill equidistant electron bunches in a storage ring, with the spin of every even (or odd) bunch flipped, while precisely monitoring the change of the beam position as asymmetry in the transverse beam spectrum in a magnetic field to access the electric dipole moment of electrons. This however would require one or more cavity BPMs operating in a ring accelerator, which is a major challenge as of the high beam coupling impedance of a cavity BPM that tends to cause beam instabilities.

The focus of this thesis is an analysis of the cavity BPM read-out electronics, in particular the RF analogue system used to downconvert and post-process the 15 GHz signal content generated by the bunched beam passing the cavity BPM pickups. Additionally, the operating principle of the CLIC cavity BPMs is presented and the performance of the setup located in the CLEAR tunnel is analyzed. For the presented beam measurements this setup was able to achieve a single bunch, single-pass resolution of $2.60\,\mu$m.

1 CLEAR and CLIC

1.1 CLIC Project

The Compact Linear Collider (CLIC) is a proposed linear electron collider for HEP research. Design and construction are managed at the European Organization for Nuclear Research (CERN), and its potential to improve the knowledge in elementary particle physics and answer some fundamental questions related to and beyond the standard model of physics are subject of an ongoing long-term study.

With a center-of-mass energy of up to 3 TeV CLIC would operate at the energy frontier for leptons, similar to the Large Hadron Collider (LHC), currently operating at 13 TeV, the energy frontier for protons. However, using electrons and positrons, i.e. point-like elementary particles for the collision instead of hadrons (LHC: protons or ions), CLIC may offer some new perspectives on todays physics. This new perspective is expected to contain higher precision as the current LHC program, as well as a better understanding in the field of physics beyond the standard model.

To achieve these high energies with a rather compact accelerator requires a high acceleration gradient of the RF cavities. For CLIC a gradient of 100 MV/m is foreseen, and was already achieved at the CLIC Test Facility (CTF).

The high gradient acceleration is provided by a two-beam acceleration scheme shown in Fig. 1. An electron beam of high intensity and low energy, the so called drive beam, is generated with help of damping and combiner rings. In 20000 Power Extraction and Transfer Structures (PETS) it is decelerated to deliver high power RF with a frequency of 12 GHz, similar to the operation of a klystron. The RF power of the drive beam is then transferred into the high gradient traveling-wave accelerating structures to accelerate the relatively low intensity main beam to high energies of up to 1.5 TeV per beam [1]. Simplistically speaking, the two-beam acceleration principle is similar to that of a transformer, a high-power, low-energy beam is "transformed" to a low-intensity, high-energy beam.

The particles in the main beam are packed in a train of up to 312 bunches, spaced by 500 ps, and each bunch contains up to $3.72 \cdot 10^9$ particles. With a train repetition rate of 50 Hz a luminosity of $5.9 \cdot 10^{34}\,\mathrm{cm}^{-2}\mathrm{s}^{-1}$ [2] is predicted. The beam parameters are shown in Tab. 1.

1.2 CLEAR Facility

To demonstrate the feasibility of the two-beam acceleration scheme, and for testing and developing the mission critical components required for CLIC the CLIC Test Facility (CTF) was built at CERN. The last upgrade of the CTF was CTF3 which was shut down in 2016.

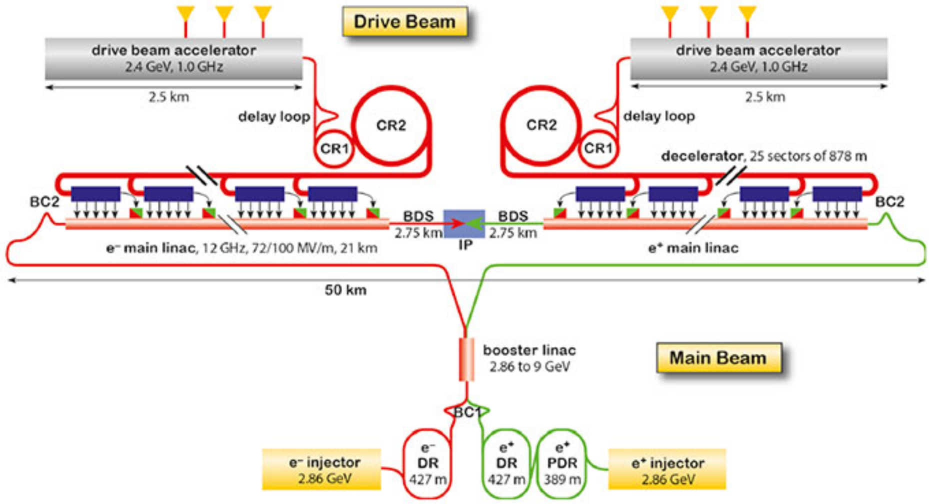

Fig. 1. Setup of the Compact Linear Collider (CLIC). A two-beam acceleration scheme is used to achieve a high acceleration gradient [1].

	CLEAR	**CLIC**
Energy	130 - 220 MeV	up to 3 TeV
Bunch charge	0.01 - 0.5 nC	0.6 nC
Repetition rate (trains)	1 - 5 Hz	50 Hz
Number of bunches in train	1 - 100	312
Bunch frequency	1.5 GHz	2 GHz

Tab. 1. Beam parameters of the CLEAR accelerator in comparison to the predicted beam parameters of CLIC [2, 3].

One part of CTF was the probe main beam line, called Concept D'Accélérateur Lineáre pour Faisceau d'Electron Sonde (CALIFES). After the finalization and shutdown of the CTF3 program, most parts of CALIFES were reused to build the CERN Linear Electron Accelerator for Research (CLEAR).

"The primary focus for CLEAR is general accelerator R&D and component studies for existing and possible future machines at CERN [2]". This covers testing of CLIC components, as well as prototyping for the LHC upgrade and high gradient acceleration methods like plasma acceleration.

Beam operation of CLEAR started in 2017, the beam parameters are shown in Tab. 1, along with the foreseen parameters of CLIC.

2 Beam Position Monitors

2.1 Motivation

The main purpose of beam position monitors (BPM) is – as the name suggests – the measurement of the beam position, i.e. the transverse displacement of the beam with respect to the center of the vacuum chamber (also called *beam pipe*). Usually the vacuum chamber has a circular, elliptical or similar symmetric cross-section, and the beam position is reported in mm or μm for horizontal x- and vertical y-axis.

Using the data of many BPMs located along the accelerator, the beam trajectory or beam orbit can be reconstructed, which is one of the most fundamental applications of a BPM system, e.g. to keep the beam on the best performing trajectory inside the vacuum chamber, sometimes called "golden orbit", and to avoid the beam touching the walls of the vacuum chamber or other sensitive accelerator components.

Especially in high energy accelerators like the LHC the continuous measurement and observation of the beam orbit is very important to prevent damage to the machine. With a total beam momentum similar to a TGV train at a speed of 150 km/h the risk of damaging the machine if the beam is too far off from the center of the beam pipe is very high.

Beside for the beam orbit, the BPMs are used for many other measurements to characterize the beam, or to understand the performance of the accelerator. BPMs are used e.g. for beam optics measurements, the measurement of beam parameters like tune, chromaticity, momentum, etc., and BPMs are also used in protection systems and for trouble shooting a faulty accelerator or transfer-line.

Particle accelerators are designed for different applications, and therefore with very different characteristics. To cope the requirements set by the accelerator and beam, several types of BPMs have been developed over the years. The focus of this thesis is on the cavity BPMs, originally designed for the CLIC project. To give an idea of their characteristics in contrast to other types of BPMs, the variety of BPM types and systems proposed for the different accelerator parts of the CLIC project are introduced in this section. Tab. 2 summarizes the characteristics of those BPM types.

2.2 Button BPMs

In accelerators and beam-lines today, the button style BPM is most commonly used. These button BPM pickups consist of a symmetric arrangement of four circular metal disks, like coins or buttons, which give them the name. The button BPM installed in the LHC is shown in Fig. 2. It is a more advanced design, as the button is also shaped with the curvature of the circular vacuum chamber.

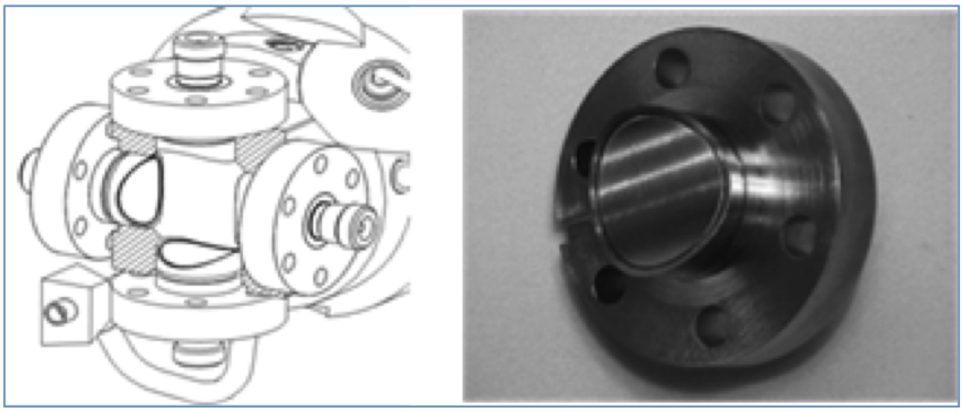

Fig. 2. The button BPMs used in the LHC [4].

Button BPMs are rather simple and robust, and therefore cost effective. For CLIC they are intended for the less challenging systems, where a resolution of up to $10\,\mu$m is required. The button BPMs will be used for example for the CLIC damping rings and the drive beam transfer lines. With the rather moderate resolution comes a low impact on the beam, which is a great advantage especially for high intensity beams.

The position of the beam is measured by comparing parts of the image charge of the beam. Each particle moving through the beam pipe produces an electromagnetic field (EM fied). At the relativistic limit $v \approx c_0$, the EM field of the charge has only transverse components (TEM field), and we can simplify the situation as a 2-dimensional electrostatic case, which causes the charged particle to induce an image charge on the conductive beam pipe walls. If the beam is in the center of a beam pipe with circular cross-section, the image charges are distributed equally. For an off-center beam the image charge distribution changes accordingly, and can be evaluated by comparing the integrated image charges, e.g. with two horizontal arranged BPM electrodes as shown in Fig. 3. As the charged particle beam moves along the beam trajectory, the image charge follows, lined through the EM-field, which allows a beam position measurement at many locations, but also enables other types of measurements, like the total charge of the beam (beam intensity measurement).

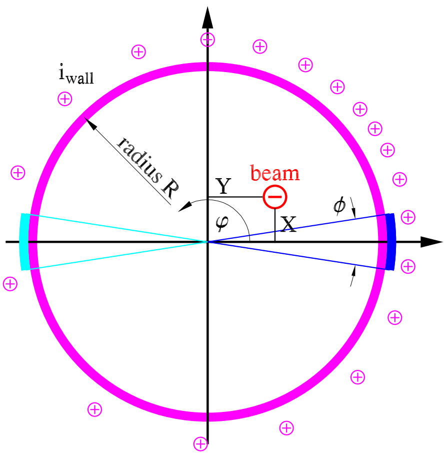

Fig. 3. Illustration of the image charge of a two-pickup BPM measuring the image charge to determine the x- and y-position of the beam.

A BPM system based on button pickups usually consists of four pickup electrodes, mounted in a symmetric, and orthogonal arrangement to supply the horizontal and vertical beam position. While for an electromagnetic point of view the arrangement of the button electrodes along the horizontal and vertical axis is preferable, this setup often has issues with synchrotron radiation in the horizontal plane and/or suffers from particle spill. The simple way out of the trouble is to "rotate" all electrodes by 45°, see Fig. 4.

With this setup the beam position is calculated as

$$\text{horizontal: } x = \frac{1}{s} \cdot \frac{(U_1 + U_4) - (U_2 + U_3)}{U_1 + U_2 + U_3 + U_4} \tag{1}$$

$$\text{vertical: } y = \frac{1}{s} \cdot \frac{(U_1 + U_2) - (U_3 + U_4)}{U_1 + U_2 + U_3 + U_4}, \tag{2}$$

where s is a scaling factor and U_i the voltage measured between ground and the ith electrode.

2.3 Stripline BPM

Similarly stripline BPMs probe the image current to measure the position of the beam. They differ from button BPMs by the pickup design, and may also have different readout electronics.

The pickups have a shape similar to a wire or strip stretched parallel to the beam direction. The extension in beam direction enables a better controlled coupling to the bunched beam, and also the possibility to distinguish counter propagating beams. This makes stripline BPMs particularly suitable for bunched beams in linear and ring colliders, with a bunch length $l_{bunch} \leq l_{strip}$. Fig. 5 shows a sketch of a stripline BPM and its readout.

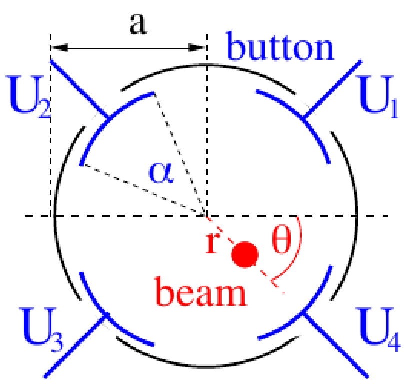

Fig. 4. Scheme of an arrangement of pickups for button BPMs [5].

As Fig. 6 indicates, the signal response of the stripline to a short bunch is a doublet pulse, with the positive (red) and negative (green) parts of the signal spaced by $2l_{strip}$ at the upstream port (port 1), while the induced signals cancel at the downstream port (port 2: no signal).

For CLIC, stripline BPMs are foreseen for the drive beam decelerator beam-lines. Here a resolution of 2 μm is required. The length of the striplines used as pickups is specified to 25 mm. Here the idea followed is related to the fact, with a bunch repetition rate of $t_{rep} = 2\,l_{strip}/c_0$, the signal traveling back from port 2 and the following bunch signal cancel, such that only the first and the last pulse of the train remain [5]. In this way the presence of high power RF signals nearby can be effectively suppressed, while staying sensitive to the beam signal.

2.4 Cavity BPMs

In contrast to stripline and button BPMs, cavity BPMs do not follow the image current principle to measure the beam position. They use the signal amplitudes of the eigenmodes, which a beam excites inside a cavity resonator when passing off center.

Typically, the cavity BPMs are designed on basis of a simple cylinder with circular cross-section, sometimes called “pillbox” cavity, with metallic walls and a port hole in each end to pass the beam.

The amplitude of the lowest dipole eigenmode depends on the beam offset, but it is also dependends on the beam charge, while the amplitude of the lowest monopole eigenmode is used to normalize the dipole mode signal to the beam charge, and to reference the dipole mode phase. As the monopole mode and the dipole mode, both operating at the same frequency have to be measured, two cavities are required. Moreover, the dipole mode has two polarizations, which are used for horizontal and vertical beam position measurement, therefore three read-out systems are required at minimum.

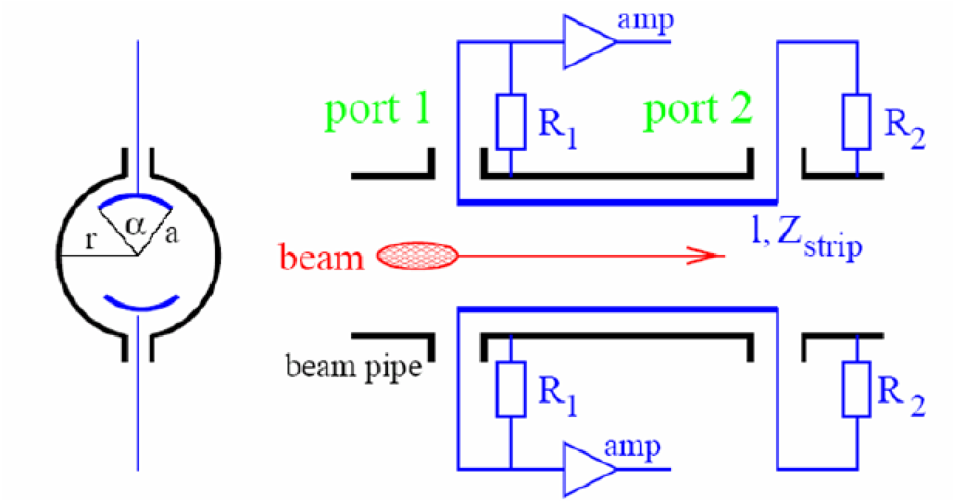

Fig. 5. Sketch of the pickups and readouts of a stripline BPM [5].

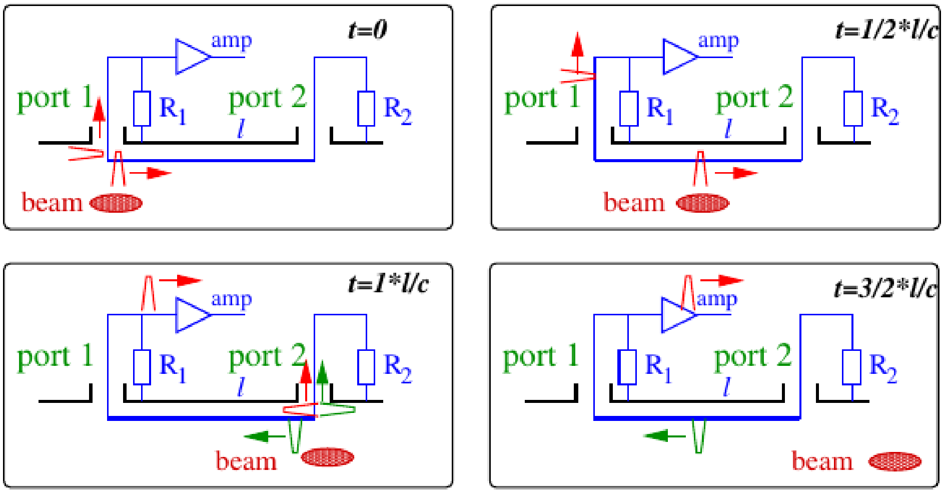

Fig. 6. Visualization of the signal generation of a stripline BPM

For CLIC, cavity BPMs are intended for the main LINAC and the beam delivery system. Here a spatial resolution of 50 nm and a temporal resolution of 50 ns is requested. These high resolutions can only be provided with cavity BPMs.

However, the cavity BPMs has the downside of a limited frequency bandwidth, for which they are able to provide high resolution beam position data. Also, as of strong beam coupling, the so-called coupling impedance of a cavity BPM is large, which disqualifies their usage in ring accelerators. Furthermore, the signal processing is comparably sophisticated. These characteristics limit their usage to linear accelerators, currently only FEL-based light sources like LCLS at SLAC, and FLASH2 and XFEL at DESY, use them in day-to-day operation. In the next sections the theory behind the cavity BPMs is described, and the design, the readout electronics, and the performance potential of the cavity BPMs designed for CLIC are presented.

BPM Type	**Pros and Cons**
Button	+ Simple, robust and inexpensive − Moderate resolution (10 μm)
Stripline	+ Higher resolution (2 μm) + Integrable into other components like magnets + Directional − More expensive and less robust
Cavity	+ Very high resolution (50 nm) − Limited time resolution − Sophisticated and expensive − Not applicable for ring accelerators

Tab. 2. Summary of the characteristics of the different BPM types proposed for the CLIC project.

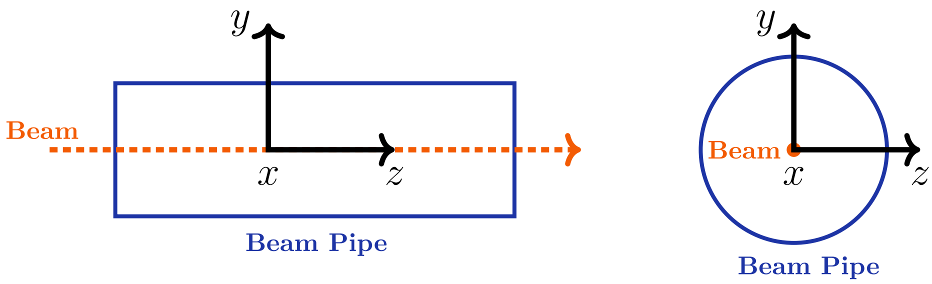

Fig. 7. Coordinate system used in the whole thesis. z represents the ideal beam trajectory, x the horizontal and y the vertical coordinate.

3 Theory

In this section the eigenmodes of an ideal cavity are derived as it is not possible to derive the eigenmodes of the real cavity with analytical methods. In a next step the characteristics of a cavity are explained using equivalent circuits.

An ideal cavity is a pillbox filled with vacuum and made of an ideal conductor. In contrast to real cavities it does not have holes for the beam or readout ports.

The coordinate system, which is used for the theory as well as for the following chapters is shown in Fig. 7. The beam pipe is assumed to be a circular shaped pipe. The z-axis is in the center of this pipe representing the ideal beam trajectory. Cutting the beam pipe perpendicular to the z-direction the x-axis is the horizontal coordinate and the y-axis the vertical coordinate.

3.1 The eigenmodes of an ideal cavity

From Maxwell's Equations in vacuum

$$\nabla \cdot \boldsymbol{H} = 0 \tag{3}$$

$$\nabla \times \boldsymbol{H} = \epsilon_0 \frac{\partial \boldsymbol{E}}{\partial t} \tag{4}$$

$$\nabla \cdot \boldsymbol{E} = 0 \tag{5}$$

$$\nabla \times \boldsymbol{E} = -\mu_0 \frac{\partial \boldsymbol{H}}{\partial t} \tag{6}$$

we can derive the wave equations for the electric and magnetic field

$$\left(\boldsymbol{\nabla}^2 - \frac{1}{c^2}\frac{\partial^2}{\partial t^2}\right)\boldsymbol{E} = 0 \tag{7}$$

$$\left(\boldsymbol{\nabla}^2 - \frac{1}{c^2}\frac{\partial^2}{\partial t^2}\right)\boldsymbol{H} = 0. \tag{8}$$

$\boldsymbol{H}$ is the magnetizing field, $\boldsymbol{E}$ the electric field, ϵ_0 the permittivity of free space, μ_0 the permeability of free space and c the speed of light with $c = 1/\sqrt{\mu_0\epsilon_0}$. Assuming that $\boldsymbol{E}(\boldsymbol{r},t)$ and $\boldsymbol{H}(\boldsymbol{r},t)$ are waves with frequency ω, the electric and magnetic field and the wave equations have the following form.

$$\boldsymbol{E}(\boldsymbol{r},t) = \boldsymbol{E}(\boldsymbol{r})\mathrm{e}^{i\omega t} \tag{9}$$

$$\boldsymbol{H}(\boldsymbol{r},t) = \boldsymbol{H}(\boldsymbol{r})\mathrm{e}^{i\omega t} \tag{10}$$

$$\boldsymbol{\nabla}^2\boldsymbol{E}(\boldsymbol{r}) + \frac{\omega^2}{c^2}\boldsymbol{E}(\boldsymbol{r}) = 0 \tag{11}$$

$$\boldsymbol{\nabla}^2\boldsymbol{H}(\boldsymbol{r}) + \frac{\omega^2}{c^2}\boldsymbol{H}(\boldsymbol{r}) = 0. \tag{12}$$

Instead of directly applying all boundary conditions for a pillbox, the equations above are at first solved for a waveguide in z-direction and afterwards the boundary conditions for two walls made from an ideal conductor installed perpendicular to the z-direction are added. To solve the wave Eq. 11 and 12 the ansatz of a plane wave moving in z-direction is used [6] where k is the wave number. This gives

$$\boldsymbol{E}(\boldsymbol{r}) = \boldsymbol{E}(r,\varphi)\mathrm{e}^{ikz} \tag{13}$$

$$\boldsymbol{H}(\boldsymbol{r}) = \boldsymbol{H}(r,\varphi)\mathrm{e}^{ikz} \tag{14}$$

$$\boldsymbol{\nabla}\boldsymbol{E}(r,\varphi) + k_c^2\boldsymbol{E}(r,\varphi) = 0 \tag{15}$$

$$\boldsymbol{\nabla}\boldsymbol{H}(r,\varphi) + k_c^2\boldsymbol{H}(r,\varphi) = 0 \tag{16}$$

with

$$k_c^2 = \frac{\omega^2}{c^2} - k^2.$$

Eq. 15 and 16 can be solved by the following separation.

$$E_z(\boldsymbol{r}) = R_E(r)\Theta_E(\varphi) \tag{17}$$

$$H_z(\boldsymbol{r}) = R_H(r)\Theta_H(\varphi) \tag{18}$$

with

$$\Theta(\varphi) = A\cos(m\varphi) + B\sin(m\varphi) \tag{19}$$

$$R(r) = CJ_m(k_c r) + DN_m(k_c r). \tag{20}$$

J_m are the Bessel functions and N_m are the Neumann functions.

The fields inside the waveguide have to be continuous. The Neumann Functions N_m are singular at $r = 0$ which is inside the waveguide. Therefore D has to be set to zero [6]. At the wall of the waveguide is a transition from vacuum to the ideal conductor. From Maxwell's Equation we get additional boundary conditions for this transition. The parallel components of the electric field and the perpendicular components of the magnetic field have to vanish. Therefore we have the following conditions for the fields in the waveguide at $r = a$ where a is the inner radius of the waveguide:

$$H_r = 0 \tag{21}$$

$$E_z = 0 \tag{22}$$

$$E_\varphi = 0. \tag{23}$$

To comply with these conditions either E_z or H_z has to be zero for all r. To explain why H_z is zero for the cavity BPMs one has to take a look at the way the eigenmodes are excited by the beam. The beam is a current in z-direction producing an electric field in z-direction. Following this, modes with a vanishing z-component in the electric field will not be excited. From this follows that the modes in the cavity have a vanishing z-component in the magnetic field. To meet the boundary conditions 21-23, the Bessel functions have to be zero at $r = 0$. Putting everything together yields into the following moving wave.

$$E_z = E_{mn} \cdot J_m(k_c r) \cdot \mathrm{e}^{im\varphi} \mathrm{e}^{ikz} \mathrm{e}^{i\omega_{mnp} t} \tag{24}$$

with

$$J_m(k_c a) = 0,$$

where m and n are natural numbers representing the number of wave nodes in φ and r direction.

To obtain the electric field inside a cavity, walls made of an ideal conducting material are inserted at $z = \pm l$ with $k = p \cdot \frac{\pi}{l}$. The moving wave described by Eq. 25 has nodal planes at l. Therefore the inserted walls transform the moving wave into the standing wave [6]

$$TM_{mnp} : E_z = E_{mn} \cdot J_m(k_c r) \cdot \mathrm{e}^{im\varphi} \cos(i \frac{p\pi}{l} z) \mathrm{e}^{i\omega_{mnp} t} \tag{25}$$

with

$$J_m(k_c a) = 0.$$

The two modes used for beam position measurements are the monopole mode TM_{010} shown in Fig. 8 and the dipole mode TM_{011} shown in Fig. 9.

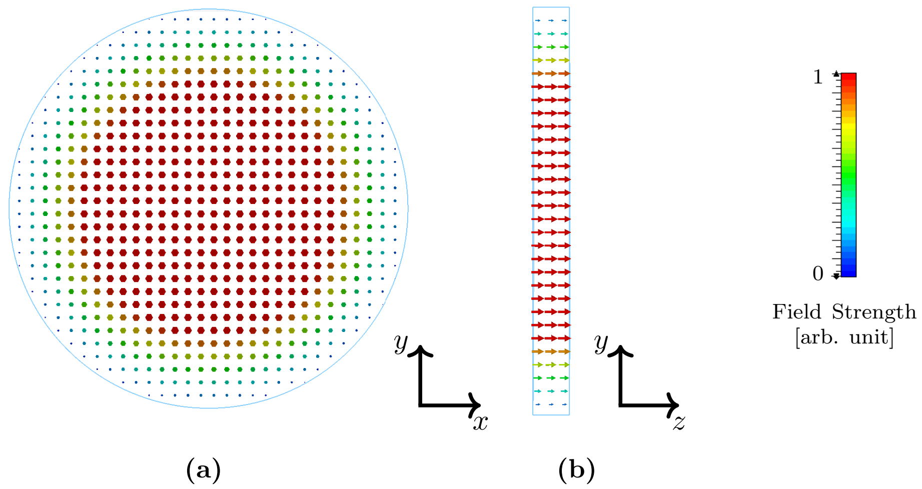

Fig. 8. Electric field of the monopole mode TM_{010} at $t = 0$. Cut through the x-y-plane at $z = 0$ (a) and cut through the y-z-plane at $x = 0$ (b).

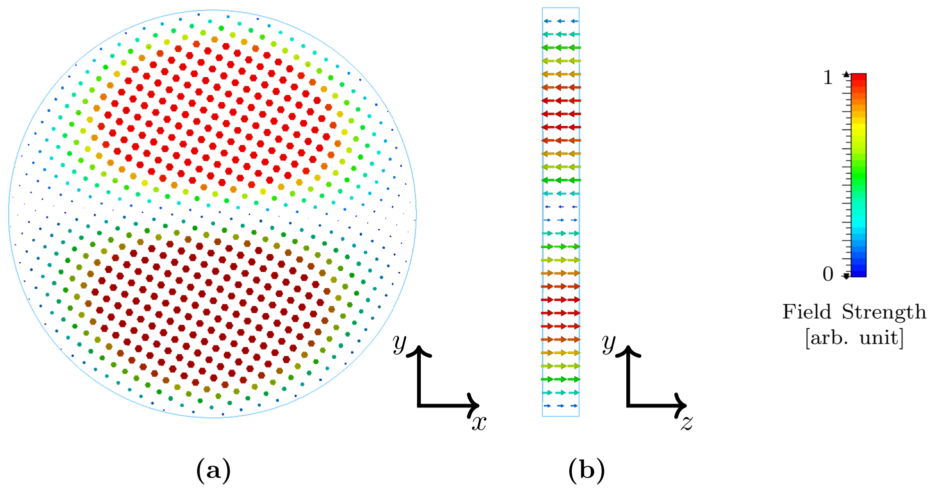

Fig. 9. Electric field of the dipole mode TM_{110} at $t = 0$. Cut through the x-y-plane at $z = 0$ (a) and cut through the y-z-plane at $x = 0$ (b).

3.2 Characteristics of the Pickup

Each of the eigenmodes can be represented by an equivalent circuit, which is able to produce the signal of this eigenmode. In the following this is used to describe the characteristics of the BPM pickup.

The equivalent circuit of a cavity without the beam or a connected load is a damped oscillating circuit consisting of a capacitor, a resistor and a coil connected in parallel like the one shown in Fig. 10. The values of the components define which eigenmode is produced.

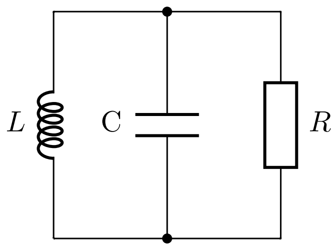

Fig. 10. Equivalent circuit of the pickup.

3.2.1 The Generated Signal

The first of Kirchhoff's laws describes, that in every point in a circuit the incoming current is equivalent to the outgoing current

$$\sum_{k=1}^{n} I_k = 0. \tag{26}$$

For the presented circuit this presets:

$$-I_L = I_R + I_C \tag{27}$$
$$\Rightarrow -\dot{I}_L = \dot{I}_R + \dot{I}_C. \tag{28}$$

The second Kirchhoff's law says that in a closed circuit the sum over all voltages is zero

$$\sum_{k=1}^{0} V_k = 0. \tag{29}$$

From this follows for the oscillation circuit:

$$V := -V_L = V_R = V_C \tag{30}$$

with

$$V_L = L \cdot I_L \tag{31}$$
$$V_R = R \cdot I_R \tag{32}$$
$$V_R = \frac{Q_C}{C}. \tag{33}$$

Put together, Eq. 28 and 31 result into the homogeneous linear differential equation

$$\ddot{V} + \frac{\dot{V}}{CR} + \frac{V}{CL} = 0. \tag{34}$$

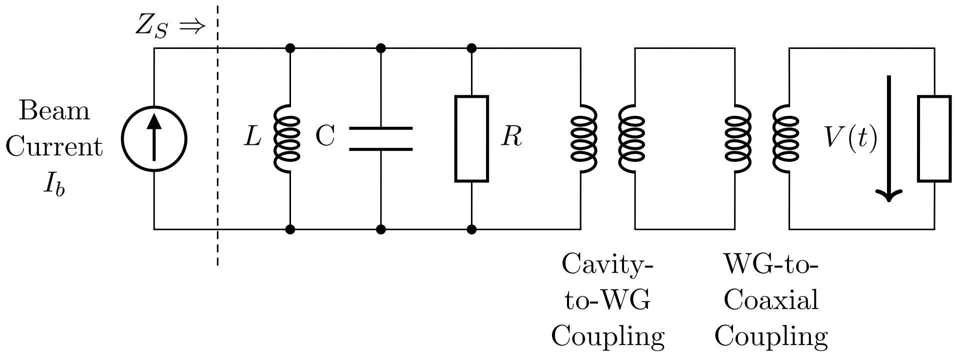

Fig. 11. Equivalent circuit of the cavity pickup with a current source representing the beam and a transformer representing the waveguide coupling [7].

To solve this differential equation the ansatz $V(t) = V_0 \mathrm{e}^{\lambda t}$ is used. Inserting it into Eq. 34 one gets

$$\lambda = -\frac{\tau}{2} \pm \sqrt{\frac{\tau^2}{4} - \omega_0^2}, \tag{35}$$

where $\tau = 1/CR$ is the decay time and $\omega_0 = 1/\sqrt{CL}$ the resonance frequency. Assuming that the decay time is small in comparison to the resonance frequency, one can approximate $\tau^2/4 - \omega_0^2 \approx \omega_0^2$ [6]. The signal produced by an ideal cavity is therefore

$$V(t) = V_0 \mathrm{e}^{-\frac{\tau t}{2}} \mathrm{e}^{i\omega_0 t}. \tag{36}$$

3.2.2 Excitation and Signal Transmitting

Also the excitation through the beam and the signal transmitting from the pickup to the readout electronics can be illustrated with equivalent circuits. The circuit including the excitation and the signal transmitting is shown in Fig. 11. The beam is a current source and the coupling between the BPM pickup and the waveguide as well as the coupling between the waveguide and the coaxial cable are represented by transformers.

The shunt impedance Z_S is a parameter of a resonator. It gives the proportionality between the power taken from the beam and the square of the beam current.

$$P = \mathrm{Re}(Z_S) \cdot I_b^2 \tag{37}$$

and therefore also

$$V(t) \propto Z_S \cdot I_b. \tag{38}$$

A higher shunt impedance complies with higher sensitivity but it comes with the disadvantage of higher beam impact.

3.3 Pulse Shape of the Beam

The cavities in the BPM pickups are adjusted to 15 GHz, which is the tenth harmonic frequency of the bunch spacing frequency of 1.5 GHz in CLEAR. However, to simplify troubleshooting and analysis, all beam measurements (see Sec. 6) are performed using single bunched beams. In CLEAR this complies with a bunch frequency of around 1 Hz but it is still possible to excite the eigenmodes in the BPM cavities.

The following calculations show, that even if there is no micro bunching within the bunches, a Gaussian shaped bunch and also a digital signal are able to excite the eigenmodes.

3.3.1 Pulse with Gaussian Shape

A Gaussian pulse has the following form

$$\varphi(t) = \frac{1}{\sqrt{2\pi\sigma^2}} \mathrm{e}^{-\frac{t^2}{2\sigma^2}}. \tag{39}$$

To examine the contributions of the different frequencies the pulse is transformed into frequency domain by performing a Fourier transformation:

$$\hat{\varphi}(\omega) = \int_{-\infty}^{\infty} \varphi(t) \mathrm{e}^{-i2\pi t\omega} dt \tag{40}$$

$$= \int_{-\infty}^{\infty} \frac{1}{\sqrt{2\pi\sigma^2}} \mathrm{e}^{-\frac{t^2}{2\sigma^2}} \mathrm{e}^{-i2\pi t\omega} dt \tag{41}$$

$$= \frac{1}{\sqrt{2\pi\sigma^2}} \sqrt{2\pi\sigma^2} \mathrm{e}^{-2\pi^2\omega^2\sigma^2}. \tag{42}$$

The pulse length σ at CLEAR ranges from 0.5 μm to 1.2 mm corresponding to 1.6 ps to 4 ps. For a pulse length of 1.6 ps one gets:

$$\hat{\varphi}(15\,\mathrm{GHz}) = 0.99 \tag{43}$$

and for a pulse length of 4 ps:

$$\hat{\varphi}(15\,\mathrm{GHz}) = 0.93. \tag{44}$$

This shows that a beam with single bunches is able to excite oscillations inside the cavity. Following this, a single bunched beam can be used for beam measurements with the cavity BPMs.

3.3.2 Digital Pulse

The same analysis is performed for a digital signal. In time domain the pulse looks like

$$\varphi(t) = \theta(t) - \theta(t+\sigma). \tag{45}$$

In frequency domain this is:

$$\hat{\varphi}(\omega) = \int\limits_{-\infty}^{\infty} \theta(t) - \theta(t+\sigma)dt \tag{46}$$

$$= \int\limits_{-\infty}^{\infty} \theta(t) - \theta(t+\sigma)dt - \int\limits_{-\infty}^{\infty} \theta(t)dt \tag{47}$$

$$= \frac{1}{2}(\partial(\omega) - \frac{i}{\pi\omega}) - \frac{1}{2}(\partial(\omega) - \frac{i}{\pi\omega})\mathrm{e}^{-i2\pi\sigma\omega}. \tag{48}$$

Assuming $\omega \neq 0$ we get:

$$|\hat{\varphi}(\omega)| = |(\mathrm{e}^{-i2\pi\sigma\omega} - 1)\frac{i}{\pi\omega}| \tag{49}$$

$$= \sqrt{\frac{1}{2\pi^2\omega^2}(1 + \cosh(2\pi\sigma\omega))}. \tag{50}$$

From this follows that also a digital pulse excites the eigenmodes in the cavity as long as this beam has the right pulse length σ.

Fig. 12. Picture of a CLIC cavity BPM pickup.

4 CLIC cavity BPMs

The following chapter starts with describing the pickups of the cavity BPMs designed for the CLIC project and the setup which is installed in the CLEAR tunnel. In a second step the analogue and digital post-processing of the signals, which are sent by these pickups, are presented.

4.1 The Pickups

Fig. 12 is a picture of one of the pickups. In Fig. 13 the different parts of the pickup are shown as a sketch.

Each pickup consists of a position cavity, a reference cavity, the coupling waveguide for the signal of the position cavity and the readouts of both cavities.

The position cavity is the cavity, which is adjusted to the dipole mode TM_{110} and the reference cavity is the cavity, which is adjusted to the monopole mode TM_{010}. The main beam of CLIC is intended to be a multibunch beam. To get the best results for a multibunch beam it is important to adjust the cavities to a harmonic number of the bunch spacing frequency. The bunch spacing frequency at CLEAR is 1.5 GHz. The goal of the design was to adjust both cavities to 15 GHz, which is the tenth harmonic number of the bunch spacing frequency. The adjustment to a lower harmonic would simplify the analogue post-processing but the adjustment to 15 GHz offers the very important possibility to use the beam pipe to filter out unwanted frequencies.

Waveguides transport signals which have a frequency higher or equal to the so called cut-off frequency. Also the beam pipe is a waveguide and its cut-off frequency is just above 15 GHz. Therefore all higher order eigenmodes, which are also excited through the beam, are transported away through the beam pipe. In the position cavity the dipole mode and the monopole

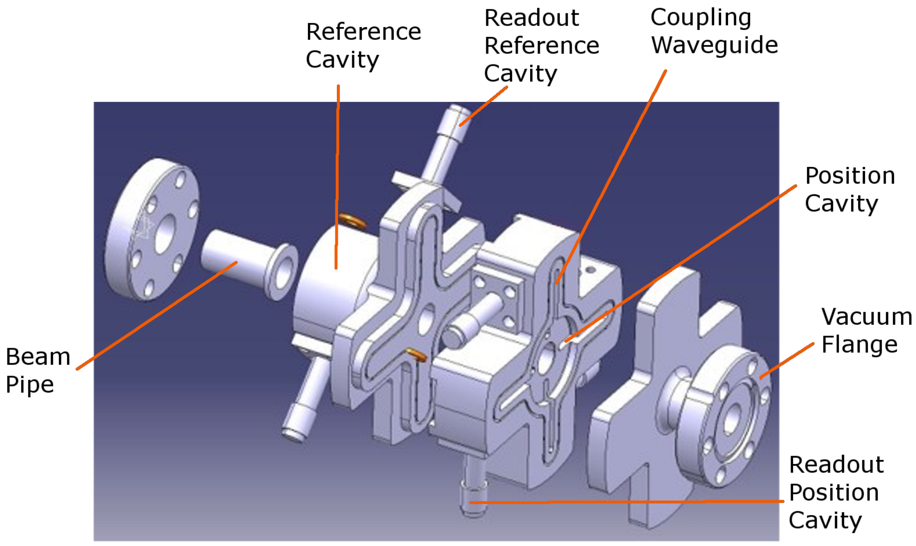

Fig. 13. Sketch of the different parts of the BPM pickup [8].

mode have frequencies below or equal 15 GHz. To prevent the monopole mode from contaminating the dipole mode signal the cut-off frequency of the waveguide, which transports the signal from the position cavity to the readout, is between the monopole mode and the dipole mode. Therefore just the signal of the dipole mode is sent through the waveguide to the readout. A further advantage of higher frequencies is the higher shunt impedance corresponding to higher sensitivity.

The reference cavity has two readout ports separated by 180 °, enabling redundant readout of the same signal. It is planned to use the redundancy for error correction. Currently one of the readout ports is used as a readin port. A 15 GHz signal can be sent into this port to simulate an eigenmode excited through the beam. Due to this calibration signal it is possible to checkout the post-processing system without having a beam passing through the cavities. The position cavity has four readout ports consisting of a redundant pair for the x- and y- direction respectively.

4.2 Tunnel Setup

Fig. 14 shows the current setup in the CLEAR tunnel. The pickup system consists of three pickups of the second generation and one of the first generation. The first generation was made from stainless steel. The Q factor for this first generation was about 250. Due to this the time resolution was even lower than required but for a spatial resolution of 50 nm a higher Q factor was required. Therefore the second generation was made from copper and some small changes in the design were applied. This second generation

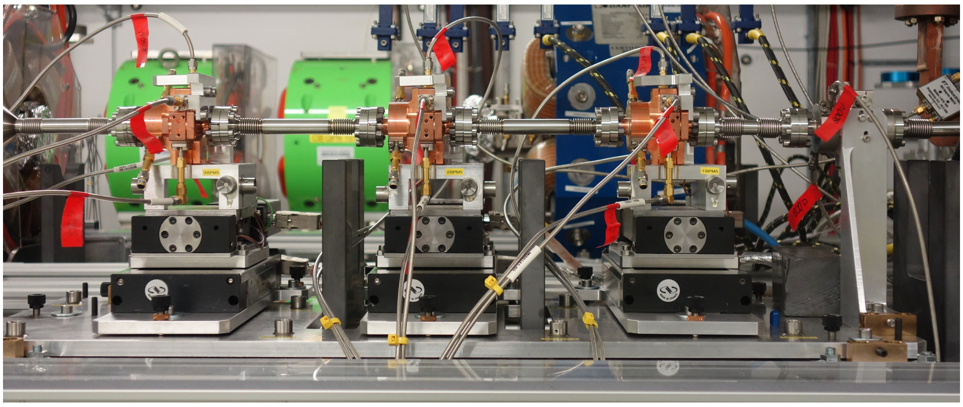

Fig. 14. Setup installed in the CLEAR tunnel. There are four pickups, three providing position cavities, and one providing a reference cavity.

reached a Q factor of about 1200. Unfortunately the resonance frequency of the reference cavities of the second generation is around 15.2 GHz, which is too far off from 15 GHz. The position cavities have a resonance frequency of about 14.987 GHz, which is close enough to the targeted 15 GHz. To get the best setup available the position cavities from the second generation are used and one pickup of the first generation is installed on the upstream side of the other pickups to provide a reference cavity. Following their function the three second generation pickups will be called position BPM and the older one reference BPM [9].

The availability of the three position measurements makes it possible to determine the resolution of the pickups. The beam is expected to be on a ballistic trajectory. This makes it possible to predict the position of one BPM knowing the positions of the two others. The resolution of the real setup can then be determined by comparing the prediction of two BPMs and the measurement of the third one. Beam measurements, which were performed to get the resolution of the current setup are presented in Sec. 6.

Each of the three position pickups are mounted on a mover table movable in x- and y-direction to simulate a beam offset, which is required for calibration (see Sec. 4.4.3).

4.3 Analog Signal Processing

As said before the signal readable at the readout ports has a frequency of roughly 15 GHz, which makes it hard to transport it with little loss and to digitize it. Therefore each readout is connected to a downmixing board (DC board) mixing down the signal to 75 MHz. Fig. 15 is a photo of one of the DC boards used.

The sketch in Fig. 16 shows the main components of the board. First the signal is sent through an amplification stage consisting of an attenuator and

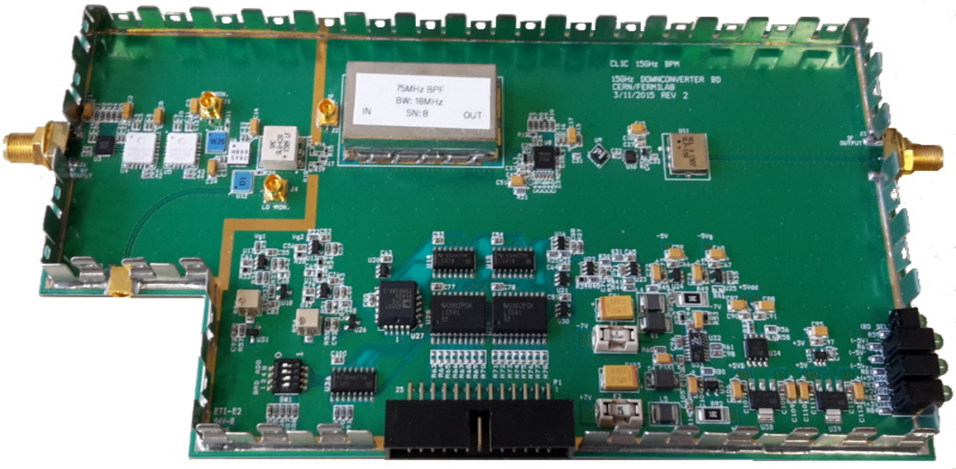

Fig. 15. Picture of a DC board used for analogue signal processing including the downconversion from 15 GHz to 75 MHz.

two amplifiers. The attenuator and the two amplifiers are tunable separately. The attenuator is controlled digitally with five bits. To control the amplifier a DAC is used to transform eight bits into a control voltage. In the following the pair of amplifiers will be called the RF amplifier. After being amplified the signal is mixed down using a mixer. To get the LO signal, which is required for this down conversion, a 233.15625 MHz signal is sent from the gallery above the accelerator tunnel and multiplied to 14.922 GHz using a dedicated PLL (phase-locked loop) board. After being mixed down the low frequency signal is filtered by a band-pass filter. The band-pass filter is followed by another amplifier, which is tunable digitally with five bits. In the following this amplifier will be called the IF amplifier. After passing a 6 dB attenuator and a 21 dB amplifier the signal is filtered by a low-pass filter and then sent into the gallery above the tunnel and there it is digitized by an Acquiris digitizer with 10 Bits and 1 GS/s.

The characteristics of this board and especially the performance of the attenuator and the amplifiers are described in Sec. 5.

In the tunnel is one box for each BPM containing a mother board and the two DC boards. The box of the first position BPM also contains the DC board for the reference BPM. The mother boards provide the required power and they have a general purpose input/output (GPIO) port to control the attenuator and the two amplifiers mentioned before.

For the beam measurements in November (see Sec. 6) the tunable components were controlled by a virtual machine running on Windows and a special controller module. A LabView program was running on the Windows computer transforming set number into a command and sending it to the controller module via Ethernet. The controller module then trans-

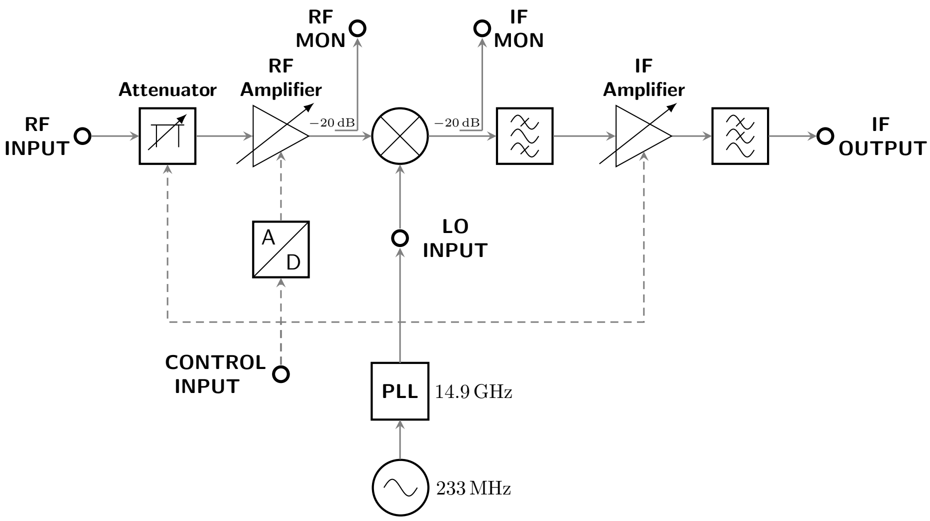

Fig. 16. A functional diagram of the main components of the analogue signal processing. Two tunable amplifiers and a tunable attenuator can be used to adapt the signal power. The mixer mixes the signal to 75 MHz and two filters are used to improve the signal.

formed this command into the corresponding combination of powered GPIO pins, which were connected to the GPIO port of the BPM boxes. However these setup had some issues. Fig. 17 shows the number set in the LabView program and the amplification, which was applied setting this number for two different boards. The unexpected behaviour in the beginning is caused by controlling the amplifier with a too low control voltage (see Sec. 5) but the jumps are caused either by the LabView program or by the controller module.

As a Raspberry Pi is inexpensive and easy to use it was decided to replace the virtual machine and the controller module by a Raspberry Pi 2B. The model 2B was chosen as it is able to provide 25 GPIO pins but does not have a WLAN adapter. A Raspberry Pi with a WLAN adapter was expected to be a security risk for the Technical Network at CERN. Another reason for choosing the Raspberry Pi was already existing software for the analysis of the cavity BPM measurements. Using Raspbian as the operating system the Raspberry Pi constitutes a ready-to-use Python environment, which also simplified the automated measurements presented in Sec. 5.

The GPIO pins of the Raspberry are connected to the GPIO port of the mother board with a flat ribbon. The Python package PyGPIO provides an easy-to-use interface to control the single pins. Tuning the components on the boards requires the control of several pins in parallel. Therefore a script was written which translates intended settings into the right pin combination. Some GPIO pins of the Raspberry Pi are by default occupied

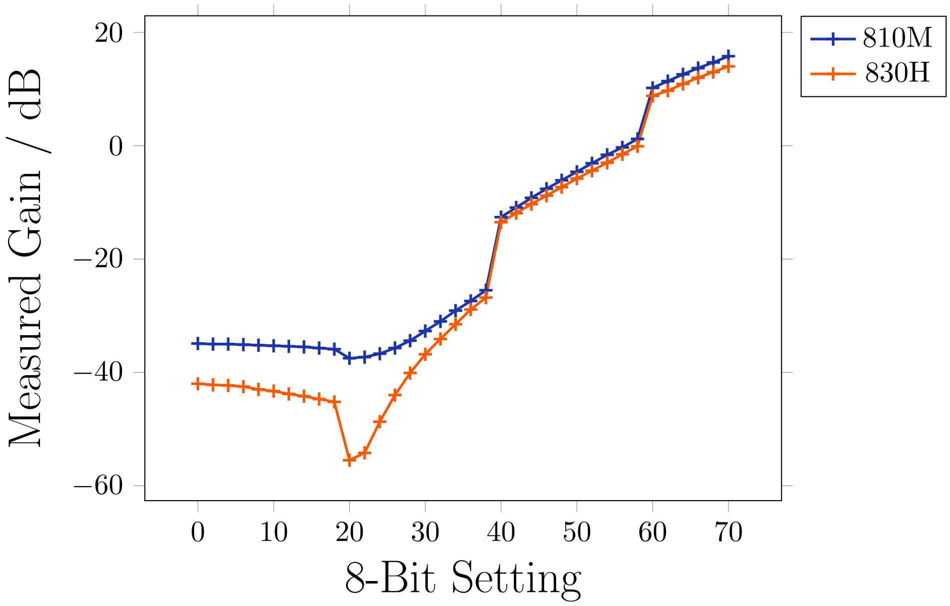

Fig. 17. The Amplification of the RF amplifier plotted against the set number. The numbers are set by dedicated controller module connected to a LabView program (Alexey Lyapin).

by protocols like I^2C. Setting up the Raspberry Pi these protocols have to be disabled to have enough GPIO pins available for the DC board.

4.4 Digital Signal Processing

The ideal digitized signal for channel i is of the form:

$$V_i[n] = u(n - n_0)Ae^{-\frac{n-n_0}{\tau f_s}} \cos(2\pi \frac{f_{IF}(n - n_0)}{\tau f_s} + \phi) \tag{51}$$

where A is the signal amplitude, f_{IF} is the signal intermediate frequency, τ is the signal decay time, f_s is the sampling frequency of the digitizer, ϕ is an unknown phase offset, n is the sample number and n_0 is the time in samples, not necessarily an integer, at which the beam-induced signal starts. $u(k)$ is the unit step function [7]. A plot of this signal for $n > n_0$ is shown in Fig. 18a. Fig. 18b shows the signal of a real beam measurement. There the oscillation needs some time to reach the maximum amplitude and the signal is superimposed by some noise.

In a first step of the digital post-processing a possible noise offset is removed. For this the mean value of the count of the first 20 samples is calculated. This mean is than subtracted from the counts of all samples belonging to this shot. Then the method of digital downconversion (DDC)

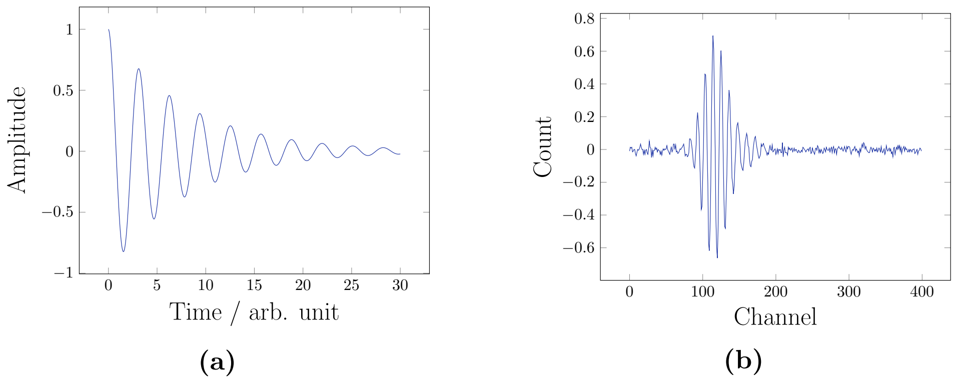

Fig. 18. Plots of the ideal digitized signal (a) and a digitized signal measured with beam (b).

is used to analyze the waveform. Here other methods like Fourier transformation would be suitable as well.

4.4.1 Digital Down Conversion

At first the signal is converted into baseband by multiplying it with the oscillator [7]

$$L[n] = 2\mathrm{e}^{i2\pi\frac{f_{IF}}{f_s}n}. \tag{52}$$

The frequency f_{IF} is determined by averaging over the frequencies of each shot gained by Fast Fourier Transformation (FFT). This multiplication results in a sum of one component which depends on the frequency 2_{IF} and one zero frequency component describing the envelope

$$V_i[n] = A\mathrm{e}^{-\frac{n-n_0}{\tau f_s}}\left[\mathrm{e}^{i(2\pi\frac{2f_{IF}}{f_s}n-2\pi\frac{f_{IF}}{f_s}n_0+\phi)} + \mathrm{e}^{-i(\phi-2\pi\frac{f_{IF}}{f_s}n_0)}\right]. \tag{53}$$

To get rid of the sum frequency component at $2f_{IF}$ a Gaussian filter of the following form is used

$$h[n] = \frac{1}{\omega\sqrt{2\pi}}\mathrm{e}^{-\frac{n^2}{2\omega^2}}. \tag{54}$$

Convoluting Eq. 53 with the Gaussian filter gives

$$V_f[n] = A\mathrm{e}^{-\frac{n-n_0}{\tau f_s}}\mathrm{e}^{-i(\phi-2\pi\frac{f_{IF}}{f_s}n_0)}. \tag{55}$$

Fig. 19 shows the real part of V_f and the original signal. Using Eq. 55 the amplitude and the phase can be determined for every sample. The amplitude is the modulus of the complex number and the phase is its argument [7].

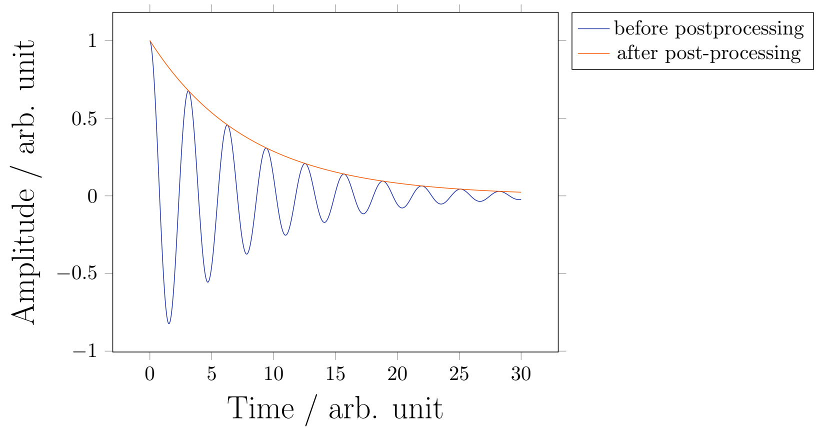

Fig. 19. The digitized signal and the real part of the signal after post-processing.

4.4.2 Application of the Reference Signal

As mentioned the amplitude of the dipole mode depends on the beam position as well as the beam charge. To extract the beam charge dependency the signal of the reference cavity is also processed using DDC. For both, the position and the reference signal the processed data is analyzed at one sample. To ensure a sample behind the peak is taken, always the sample, which is 10 samples behind the maximum amplitude, is evaluated. The value associated to this sample of the position signal is then divided by the value of the chosen sample of the reference signal. The result is a complex number and therefore it can be written as the sum of the real part I, called the inphase-component, and the imaginary part Q, called the quadrature-component

$$I + iQ = \frac{A_p}{A_r} \mathrm{e}^{\left(\frac{n_r - n_0}{\tau_r f_s} - \frac{n_p - n_0}{\tau_p f_s}\right)} \mathrm{e}^{i\left(2\pi\left(\frac{f_{IF,p} - f_{IF,r}}{f_s}\right) n_0 + \phi_r - \phi_p\right)}. \tag{56}$$

Here p indicates the position signal and r the reference signal. A is the amplitude, ϕ the phase and f_{IF} the intermediate frequency. n_r and n_p are determined within the calibration process, f_r and f_p are determined through FFT. Therefore $n_r - n_0$, $n_p - n_0$, f_r and f_p are fixed. τ_p and τ_r are also assumed to be fixed. Hence Eq. 56 just depends on the beam charge, the beam position, the trajectory angle and the bunch tilt. The dependency on the beam charge is removed by the division by A_r. The analogue LO changes the phase of the signal. This effect is canceled out by subtracting ϕ_r. To achieve a one to one mapping between the real part I and the beam position, a rotation in the complex plane by the angle θ_{IQ} is applied. Then the position can be determined by

$$P = S_p \mathrm{Re}[(I_{rot} + iQ_{rot})\mathrm{e}^{-i\theta_{IQ}}]. \tag{57}$$

The rotation angle θ_{IQ} and the scaling factor S_p have to be determined by calibration measurements. Q_{rot} now contains the contribution of the beam trajectory angle and the beam tilt. For the measurements in Sec. 6 Q_{rot} is not considered.

4.4.3 Calibration Measurement

Determination of θ_{IQ} and S_p As θ_{IQ} and S_p are different for each channel the following calibration process is performed for every cavity and for each direction, i.e. horizontal and vertical to the beam direction.

In the system of the cavities moving the cavities relative to the beam is the same as moving the beam relative to the cavities. Therefore the movers can be used to simulate a known beam offset. To gain the required data the respective mover moves the cavity to equally distant positions within a given range and for each position some shots are taken and processed using DDC as described before.

I and Q, which are calculated during the DDC process, are then plotted against the corresponding position of the mover. In this plot a straight line is fitted for I and Q respectively. The angle between the line fitted for Q and the x-axis is then θ_{IQ}.

Then for both fitted lines a rotation by θ_{IQ} is applied. Due to this rotation Q becomes independent from the beam position and the I-line can be used to calculate the position if I is known. The rotated I and Q are shown in Fig. 21.

Fig. 20 shows an I-Q-plot obtained from beam measurements in June 2018 (see Sec. 6.2). The spread between the different points measured for one mover position is caused by the quadrature sum of the beam jitter and noise.

Determination of n_p To get the sample, which should be evaluated to get the beam position, for each shot of one channel, the sample with the maximum count is determined and the mean of these maximum samples is calculated. To ensure the decreasing side of the signal is analyzed, the sample 10 samples behind the mean maximum sample is chosen.

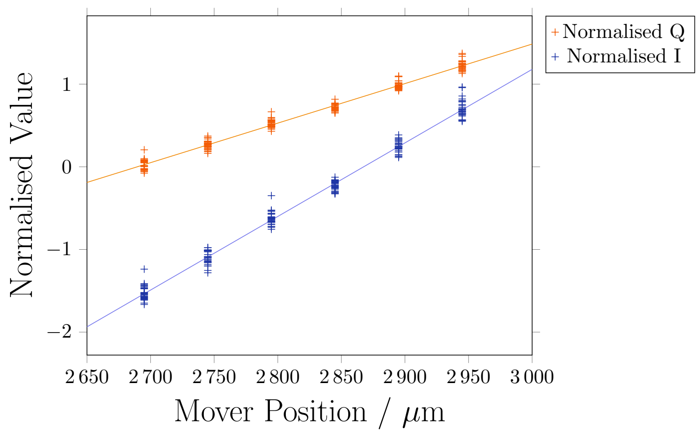

Fig. 20. I and Q calculated using Eq. 56 are plotted against the mover position and a straight line is fitted for I and Q respectively.

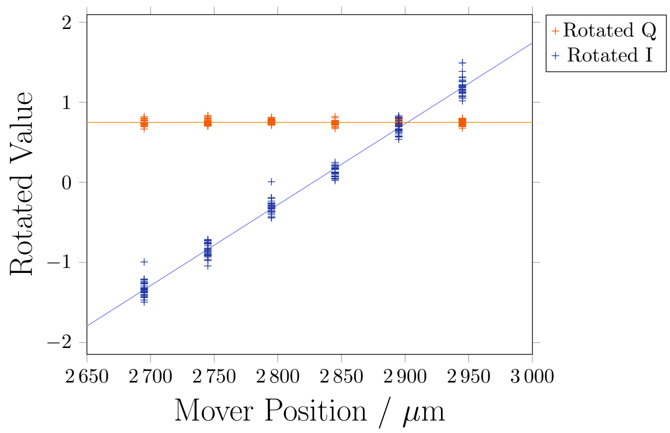

Fig. 21. I and Q rotated by the rotation angle θ_{IQ}. Q is now independent from the beam position, while I can be used to calculate the position knowing the rotated I.

5 Characterization of the DC Board

The main goal of the characterization of the DC board is to ensure that all components are tuned to the best possible settings. In order to achieve this, the working range and the impact on the signal have to be considered for each component. These characterizations will be used to write a program, which is able to provide best settings for a given beam.

During the characterization process the correlation between the 5- or 8-Bit setting and the resulting gain is measured for the attenuator, the RF amplifier and the IF amplifier. Additionally the 1 dB compression point is determined for the amplifiers and the mixer to prevent wrong results caused by saturated components.

All following measurements were performed in the lab using a spare box with two spare boards as access to the setup in the tunnel is only possible if the accelerator is shut down.

It will be assumed that the board just contains the main components shown in Fig. 16. These main components will also be charged for the small but presumably existing impacts of other components, which are not shown in the sketch but visible in the picture in Fig. 15. This assumption of a simplified board does not impair the final results as the behaviour of the board as a whole and not the behaviour of each component is significant.

Errors For the characterization of the different components no error analysis is performed as the errors on the amplification do not become errors on the beam position.

5.1 Cable attenuation

As the following measurements are performed with high frequency signals, the signal loss within the cables is not negligible. The RF INPUT and the IF OUTPUT ports of the board are SMA adapters. To connect them to the signal generator and the signal analyzer, which will be utilized for the following measurements, a Mini141 (Mini141-24 16301 1431) cable is used. Right behind the RF amplifier is the SMP port RF MON and behind the mixer is the SMP port IF MON. To connect them to the signal analyzer an Amphenol SMP to SMA cable is used followed by a Mini141.

Mini141 To determine the attenuation of the Mini141 cable, a S_{21} measurement is performed using the vector network analyzer (VNA) Agilent Technologies E5071C sweeping the signal frequency from 0 to 20 GHz in 1000 steps. To get the attenuation at 15 GHz the mean of the measured values of a width of 2 MHz around 15 GHz is taken as the value of the attenuation.

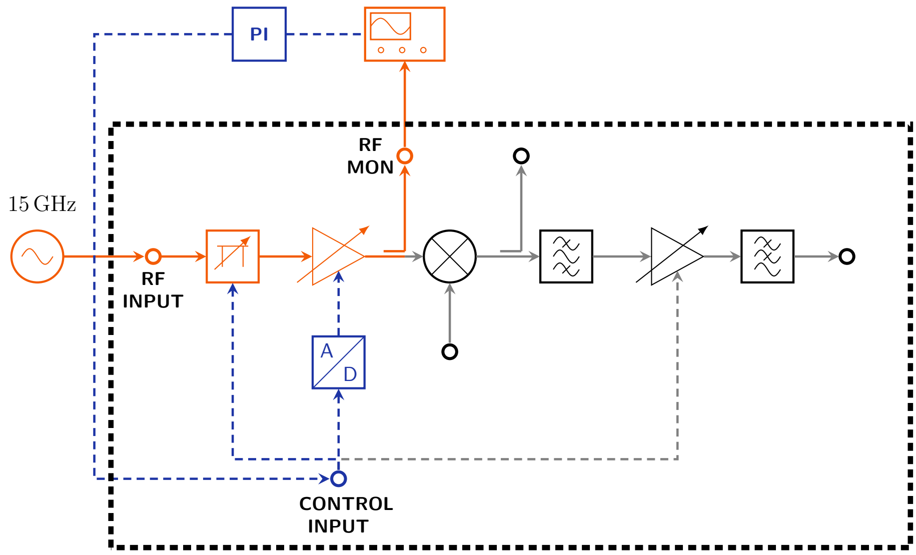

Fig. 22. Setup of the measurements for the characterization of the attenuator and the RF amplifier. The generated signal passes both components and a split part of the signal is read out at the RF MON port using a signal analyzer.

Amphenol The attenuation of the Amphenol cable is determined in the same way. For this cable the amplification is −0.78 dB.

5.2 The attenuator

The first device which is characterized is the attenuator as it is the first component in the row.

5.2.1 Setup

The setup for the characterization of the attenuator is shown in Fig. 22.

The signal generator generates a continuous 15 GHz sinusoidal signal simulating the signal sent by the BPM pickups. This signal is then fed into the RF INPUT port of the DC board and passes the attenuator and the RF amplifier. Behind the RF amplifier it is split and one part is sent to the RF MON port. Due to the splitting, the signal read out at the RF MON is attenuated by 20 dB. Both the signal analyzer and the DC board components are controlled by a Raspberry Pi. The GPIO pins of the Raspberry Pi are connected to the GPIO port CONTROL INPUT of the motherboard and the signal analyzer is controlled via USB. In Fig. 23 one can see a screenshot of a signal picked up from the RF MON port.

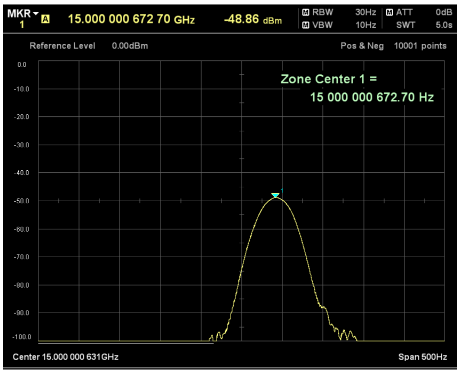

Fig. 23. Screenshot of a signal picked up from the RF monitor.

5.2.2 The Software of the Raspberry Pi

For the characterization of the amplifiers and the attenuator an automatic measurement is performed. The script is written in Python to meet the goal of having all software for the BPMs in Python. Additionally it has the advantage of being already installed on the Raspberry Pi. The whole code is appended in appendix D.

The program consists of three main parts. The components have to be tuned, the amplitude measured by the signal analyzer has to be read out and some post-processing of the obtained data is performed.

The amplifiers and the attenuator are controlled using the Python package PyGPIO as described in Sec. 4.3. For controlling and reading out the signal analyzer the Python package usbtmc is used. The USB test & measurement class (USBTMC) provides the possibility of controlling devices using commands, which are usually utilized to control a device via the general purpose interface bus (GPIB), but sending them via an USB connection. To initialize the signal generator it receives a GPIB command to load a setting, which has been set manually and saved to the memory of the signal analyzer in advance. To get the data required for the characterization the program sweeps through all possible settings, i.e. from 0 to 31 for the attenuator and the IF amplifier and from 0 to 255 for the RF amplifier. For each of these settings the signal analyzer receives a command to set a peak marker and the power level of this marker is read out.

When the program has run through all settings, each amplitude is subtracted by the input power level and the amplification of components, which are not part of the characterization, like the cables and the RF amplifier for the characterization of the attenuator. This gives the amplification caused by the component which is object of the characterization. Finally these amplifications are plotted against the associated settings and the plot and the data are saved.

Frequency	15.000000631 GHz
Span	500 Hz
RBW	30 Hz
VBW	10 Hz

Tab. 3. Settings of the signal analyzer used for the characterization of the attenuator and the RF amplifier.

5.2.3 Procedure and Results

For the characterization of the attenuator the RF amplifier is set to 57 corresponding to a control voltage of −0.70 V. This value is chosen as the amplification is not very high and it is located in the well behaving area of the amplifier (see Sec. 5.3). According to the data sheet [10] this complies with an amplification of 10 dB. The settings of the signal analyzer are shown in Tab. 3.

In this setting the attenuator is characterized by the software described in chapter 5.2.2. The Raspberry Pi tunes the attenuator from 0 to 31 and for each of these settings the amplitude measured by the signal analyzer is recorded. In order to determine the amplification this amplitude is subtracted from the signal sent by the generator. Additionally 12.32 dB, taking into account 10 dB amplification by the RF amplifier, 2.32 dB attenuation by the cables and 20 dB attenuation through the splitter, are added. To detect dependencies on the input level the measurement is performed for different signal levels. The results of the measurements are shown in Fig. 24. The given power levels are the levels set at the signal generator.

The measurements for a power level of −20 dBm and −10 dBm are almost identical. The plot of the measurement with a power level of 0 dBm deviates for low numbers. This is probably caused by saturating the RF amplifier. The curves also meet the data from the data sheet [11], which specifies a straight line from 0 dB to −30 dB. The vertical shift is caused by the signal transportation line and components, which are not characterized separately.

In the following the attenuator will be charged for this additional attenuation. One could also integrate it into the amplification applied by the RF amplifier or create a virtual attenuator. This does not impact the following results. According to the data sheet the attenuator does not change the power of the signal if it is set to 0. The virtual attenuator has then an attenuation of 0.60 dB.

5.3 The RF amplifiers

The RF amplifier is characterized in the same way with the same setup. The attenuator is set to 0. Following the results from the chapter before

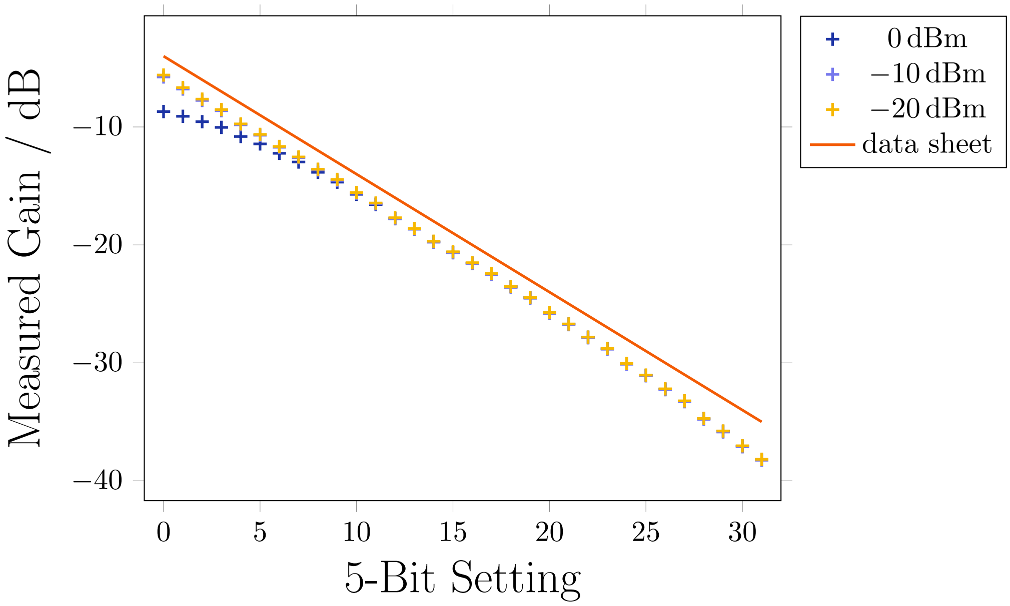

Fig. 24. Measurement of the set gain vs measured gain for the attenuator with fixed RF amplification. This measurement is performed for different signal powers. The specification of the data sheet is plotted as well.

this complies with an attenuation of 4.60 dB. The RF amplifier is tunable with 8 bits corresponding to all numbers from 0 to 255. The results of the automated measurement comparing 8-Bit setting and applied gain is shown in Fig. 25. The given power levels are the power levels set at the signal generator.

One can see, that also the behaviour of the amplifiers meets the expectations from the data sheet. In agreement to the characterization of the attenuator the curve for 0 dBm shows the typical saturation characteristic.

The unexpected behaviour in the beginning is caused by running the two amplifiers in the wrong control voltage range. According to the data sheet the lowest control voltage is −0.93 V which corresponds to a set number of 34 and an amplification of −20 dB. In the following measurements this will be the lowest setting. The highest voltage in the data sheet is 1.30 V. This is not achievable with our board. In the following measurements the highest setting is 91 as the gain difference between 91 corresponding to a control voltage of −0.36 V and 255 corresponding to a voltage of 1.28 V is less than 3 dB.

5.3.1 Linearisation

One benefit of the characterization is the availability of the data required to linearize the control of the RF amplifier. At the end of this chapter a

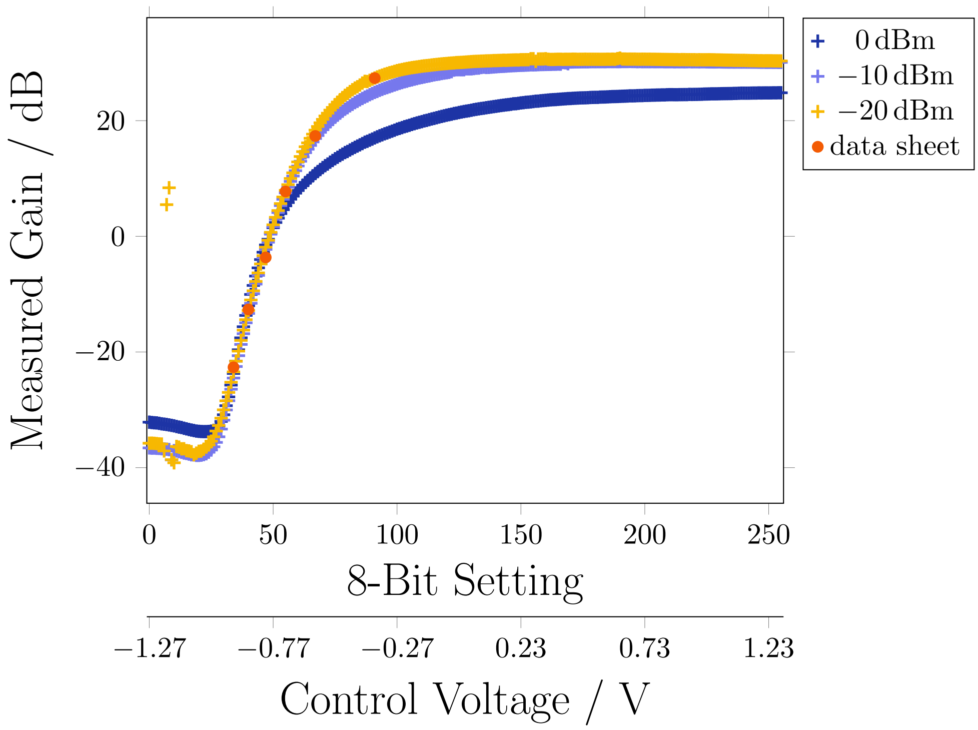

Fig. 25. Measurement of the set number versus the measured gain of the RF amplifier with attenuator set to 0 and different power levels of the generated signal. The specifications of the data sheet are plotted as well.

program is presented, which automatically finds good settings. But it may be desirable to change the settings manually. To provide an easy-to-use way a software layer basically consisting of a lookup table is added. This gives the possibility to set the amplification instead of the number corresponding to this amplification.

The results of the RF characterization with an input level of -10 dBm is used to provide the data for this lookup table. The signals recorded by the pickups have a similar or even higher amplitude. However, measurements with a higher power level would require attenuation through the attenuator. The input level of -10 dBm is a compromise between these two limitations. The program reads the data from a CSV file. From Fig. 25 one can follow that this lookup table will be sufficient for other signal levels as long as the signal power is not too high.

As in the tunnel several boards are used, one lookup table for all boards requires that different boards behave equally. Fig. 26 shows the results of using the lookup table for another board, which is available in the laboratory. The procedure of the performed measurements is equal to the measurements before but instead of comparing the set number and the measured amplification the measured amplification is compared to the amplification predicted by the lookup table. As a signal level of 0 dBm is already known to be too high, a measurement with a signal level of -5 dBm is performed instead. Additionally a level of 45 dBm is tested.

One can see that the amplifiers on different boards work similar enough to use one lookup table for all boards. The measurement with a power level of -5 dBm shows saturation characteristics.

5.3.2 Saturation

Saturation of components causes an unexpected transformation of the signal. In our measurements the saturation is visible through a decrease of the amplification. Furthermore it can damage the amplifiers running them on the limit.

A way to characterize the saturation of an amplifier is the 1 dB compression point. The 1 dB compression point is the power of the signal sent into the component, at which the real amplification is 1 dB less than the ideal behaviour. Ideally the amplifier amplifies the signal independent from the power level of the signal. Therefore the ideal curve is a horizontal line in Fig. 27, which illustrates the 1 dB compression point. The input power is plotted against the S_{21} parameter, which gives the amplification between the input port and the output port.

For the tunable amplifiers this point is dependent on the configured amplification. Therefore the 1 dB compression point is determined for several settings. For each of these settings the S_{21} parameter is plotted against the input level, which is shown in Fig. 28.

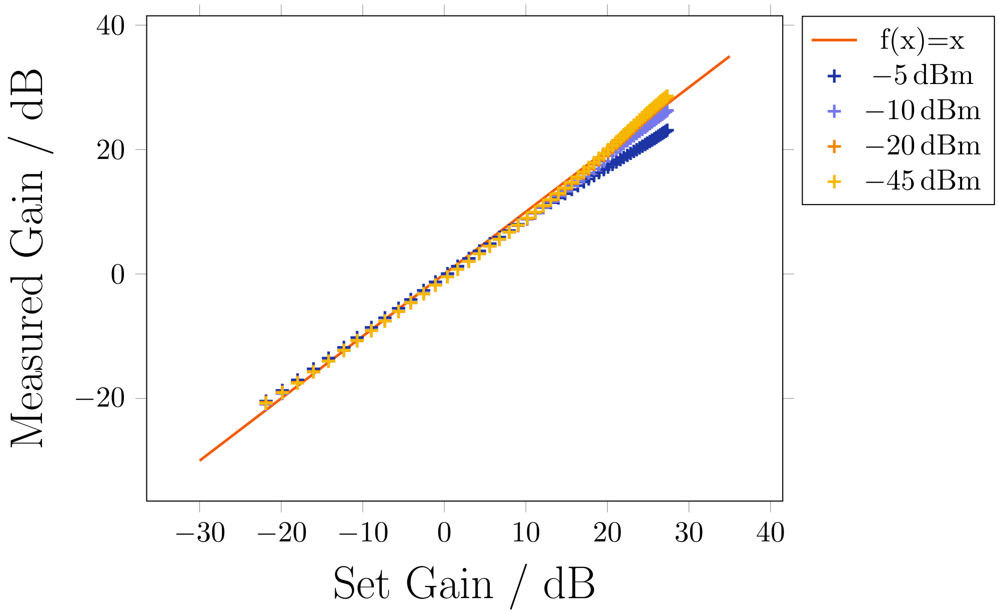

Fig. 26. Measurement to verify the lookup table with a second spare board. The set gain is plotted against the measured gain and compared to a straight line with slope 1.

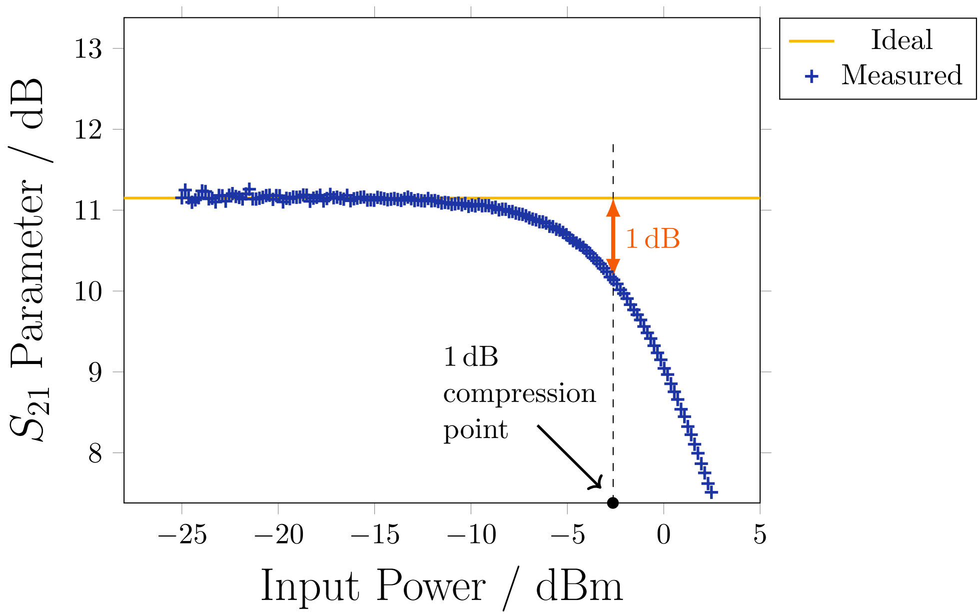

Fig. 27. Illustration of the 1 dB compression point

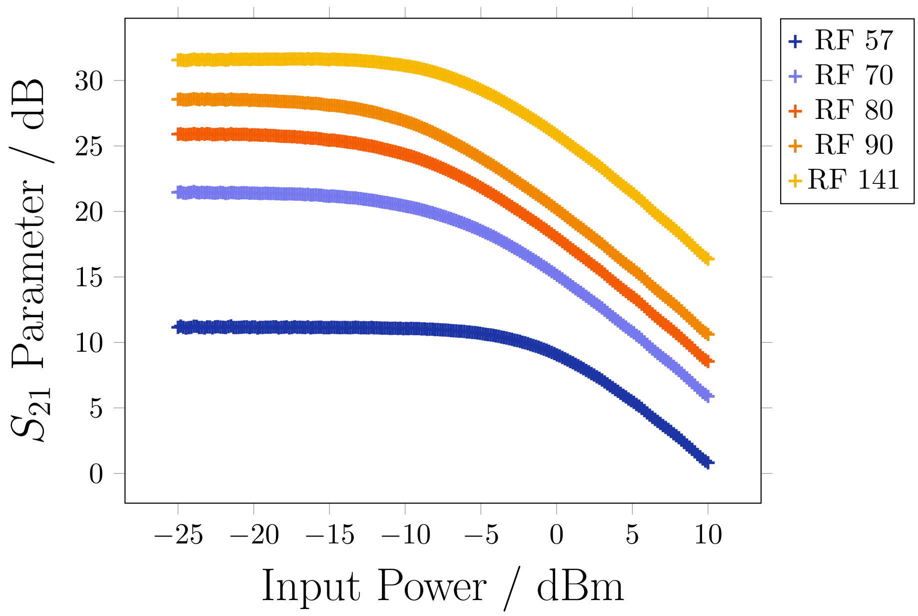

Fig. 28. S_{21} plotted against the input power to determine the 1 dB compression point. The RF amplifier is set to different amplification settings ranging from 47 to 141. In the legend RF 57 is an abbreviation for an RF setting of 57, etc./ .

The setup for this measurement is the same as in the measurement before (see Fig. 22) but the signal generator is replaced by port 1 of the network analyzer Agilent Technologies E5071C and the signal analyzer by its port 2. The frequency of the signal is 15 GHz sweeping the power level from −25 dBm to 10 dBm in 201 steps.

The determined 1 dB compression points are shown in Fig. 29a plotted against the setting of the RF amplifier. In Fig. 29b the compression points are plotted against the amplification through the RF amplifier. For settings lower than 55 no 1 dB compression point was measured in the power range examined.

The lowest compression point was −15.78 dBm. It was measured with the settings 85 and 90. The data sheet of the RF amplifier specifies a power level of 18 dBm at the 1 dB compression point at a set amplification of roughly 17 dB. This corresponds to a compression point of 2 dBm.

As described in chapter 4.3 in reality the RF amplifier consists of two amplifiers. As the output signal of the first amplifier is the input level of the second amplifier, the second one will saturate first. Having an input power of −15.78 dBm and the amplifiers are set to 90 complying with an amplification of 16.81 dB each, the input power for the second amplifier is 1.03 dBm. This meets very well the 1 dB compression point at 2 dBm deduced from the data

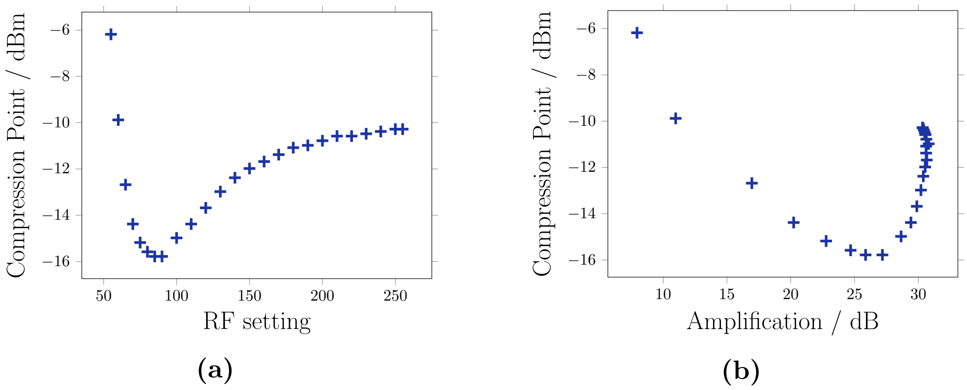

Fig. 29. The 1 dB compression point determined for the RF amplifier plotted against the corresponding setting of the RF amplifier (a) and the corresponding amplification through the RF amplifier (b).

sheet.

It is striking that for high RF settings the compression point is decreasing. The reason for this could be the chain of the two amplifiers. It is possible that the first amplifier starts to saturate for higher settings, which would lead to a lower output level which is equivalent to a lower input level for the second amplifier.

To prevent unexpected behaviour the signal sent into the RF amplifier should not be higher than −20 dBm if the whole amplification range should be used.

5.4 The Mixer

The mixer is a mixer with an amplifier inside. The amplifier is not tunable. Therefore the characterization of the mixer is just one measurement of the S_{21} parameter to determine the amplification and the 1 dB compression point.

The setup for the measurement is shown in Fig. 30. Port 1 of the VNA is connected to the RF INPUT and produces a 15 GHz signal. Port 2 of the VNA reads the signal sent to the IF MON port of the board. As this is behind the mixer, the signal has a frequency of 78 MHz.

From Sec. 4 one would expect a frequency of 75 MHz. However, the measurements assumed a signal of 15 GHz sent into the board. Mixed with a 14.922 GHz LO signal this results into a 78 MHz signal. As the band-pass filter has a band width of 20 MHz a difference of 3 MHz does not make a significant difference.

Instead of using a PLL board, the signal generator Agilent Technologies E8257D is used to provide the 14.922 GHz LO signal. It has a power level of 4 dBm. The power level of the signal sent into the RF INPUT sweeps from

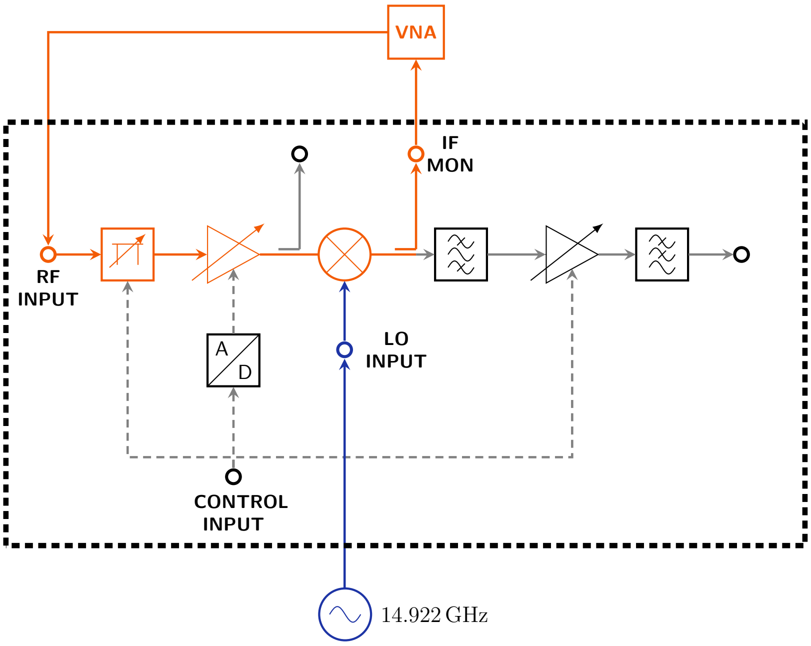

Fig. 30. Setup for the characterization of the mixer.

−35 dBm to 0 dBm.

The results of this measurement can be seen in Fig. 31. The gain of the RF amplifier, the attenuator, the cable used to connect to the IF MON port and the attenuation caused by the splitter is subtracted.

The amplification is determined by analyzing the plateau between −35 dBm and −25 dBm. The median is 11.03 dB. The data sheet [12] specifies an amplification of 11.5 dB for a temperature of 85 ° and an input frequency of 15 GHz. Following this the mixer meets the specifications in the data sheet quite well.

The 1 dB compression point is at −14.18 dBm. According to the data sheet it is at −10 dBm. The mismatch of the measurement and the data sheet could be caused by a missing power calibration. For S_{21} measurements where the signals at port 1 and port 2 have the same frequency, the VNA is able to perform a power level calibration. For a measurement with a frequency offset between the ports this is not possible and therefore some uncertainties are conceivable. Also other unknown impacts could cause the difference.

To ensure the mixer behaves as expected the signal level sent into the mixer should not exceed −18 dBm. Setting the attenuator to 0 and the RF amplifier to 57, this corresponds to a signal level of about −23 dBm at the RF INPUT port of the board.

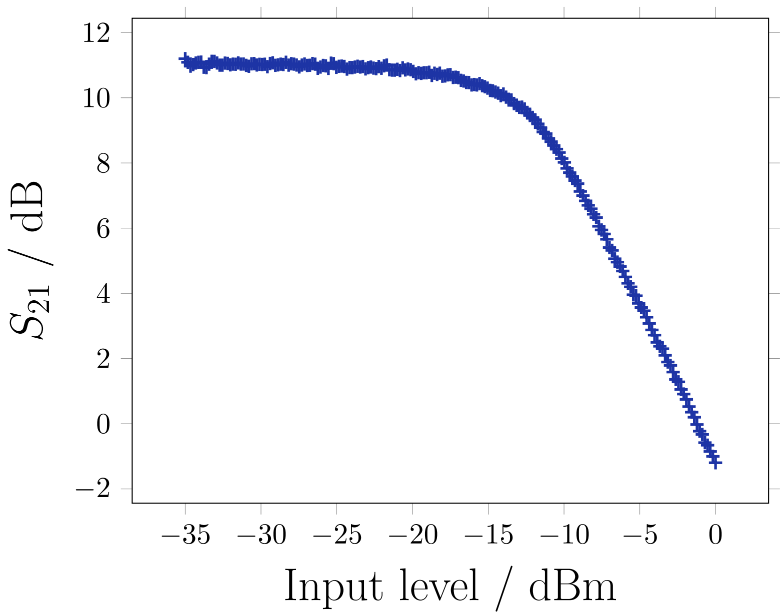

Fig. 31. S_{21} plotted against the input power to determine the 1 dB compression point and the amplification of the mixer.

Frequency	78 MHz
Span	500 Hz
RBW	30 Hz
VBW	10 Hz

Tab. 4. Settings of the signal analyzer used for the characterization of the IF amplifier.

5.5 The IF Amplifier

The IF amplifier is analyzed similarly to the RF amplifier.

5.5.1 Amplification

Fig. 32 shows the setup for the measurement of the amplification. The signal produced by the signal generator now passes the whole chain of components and is read out by the signal analyzer at the IF OUTPUT port. A second generator produces the LO signal. The settings of the signal analyzer are shown in Tab. 4. To avoid saturating the signal analyzer the power level of the signal sent into the RF INPUT port has to be reduced to −40 dBm for the automated measurement with the Raspberry Pi. The plot of the measured amplification against the 5-Bit setting is presented in Fig. 33.

For the measurement the attenuator was set to 0 and the RF amplifier

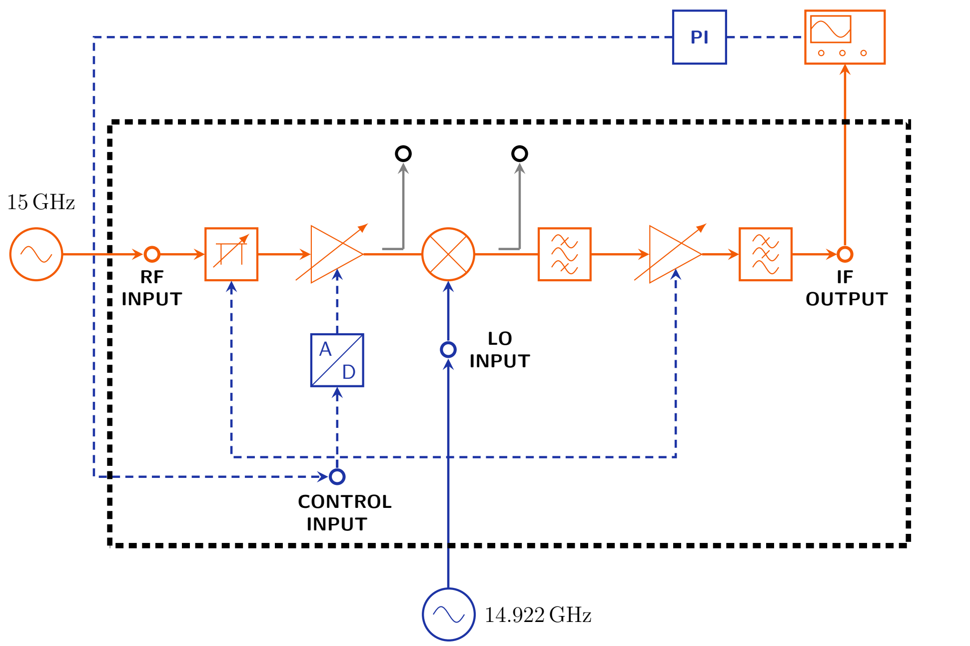

Fig. 32. Setup for characterizing the mixer.

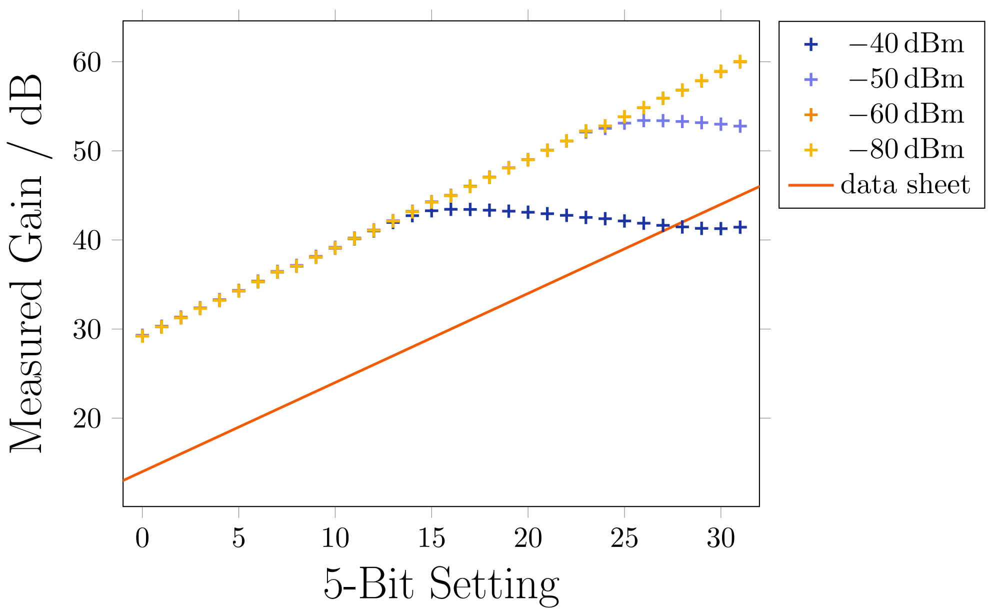

Fig. 33. The Amplification of the IF amplifier plotted against the set number assuming that between the mixer and the output is just the IF amplifier. In reality some components with fixed amplification contribute to the measured amplification.

to 57. One can see that for the different input levels the plot is almost a perfect straight line with slope 1 ranging from 29 dB to 60 dB. For the measurements with an input level of −40 dBm and −50 dBm the amplifier is saturated. However, the data sheet [13] specifies an amplification ranging from 14 dB to 45.5 dB. Following this the slope meets the specification but the absolute height is by 15 dB too high.

The reason for this discrepancy is that the measurement assumes that between the mixer and the IF OUTPUT port is just the IF amplifier but in reality the IF amplifier is followed by a 6 dB attenuator and a 21 dB amplifier.

5.5.2 Saturation

Also for the IF amplifier the 1 dB compression point is determined. The settings of the IF amplifier range from 0 to 30 in steps of 5. The setup is the same as in the measurement before but the signal generator is replaced by Port 1 of the VNA and the signal analyzer by port 2 of the VNA. To determine the 1 dB compression points for the IF settings 0,5 and 10 the power level of the signal sent to the RF INPUT port sweeps from −45 dBm to −10 dBm and for the IF settings 15, 20 and 30 from −65 dBm to −30 dBm. A 20 dB attenuator is inserted between the IF OUTPUT of the board and port 2 of the network analyzer to prevent a saturation of the network analyzer. The RF amplifier is set to 57 and the attenuator to 0.

Fig. 34 shows the curves measured for the settings 0, 5 and 10. The amplification of the components before and the attenuation applied by the 20 dB attenuator are already subtracted. Fig. 35 shows the 1 dB compression points plotted against the setting of the amplifier. In these figures the input power is the signal power sent by the VNA.

As mentioned before the IF amplifier is followed by a 6 dB attenuator and a 21 dB amplifier. It can be expected that the 21 dB amplifier saturates at first. In its data sheet [14] the output power for the 1 dB compression point is specified with 20.4 dBm. Therefore the 1 dB compression point is roughly at 1.4 dBm. The 1 dB compression point determined for IF 30 is −51.35 dBm. This corresponds to a signal level at the input of the IF amplifier of −34.92 dBm. According to the data sheet IF 30 corresponds to an amplification of 43.5 dB. The IF amplifier is followed by a 6 dB attenuator. Following this the input power at the last amplifier is 2.58 dBm, which is near to the data sheet prediction.

Concluding the calculations above the input power for this last amplifier should not exceed −3 dBm.

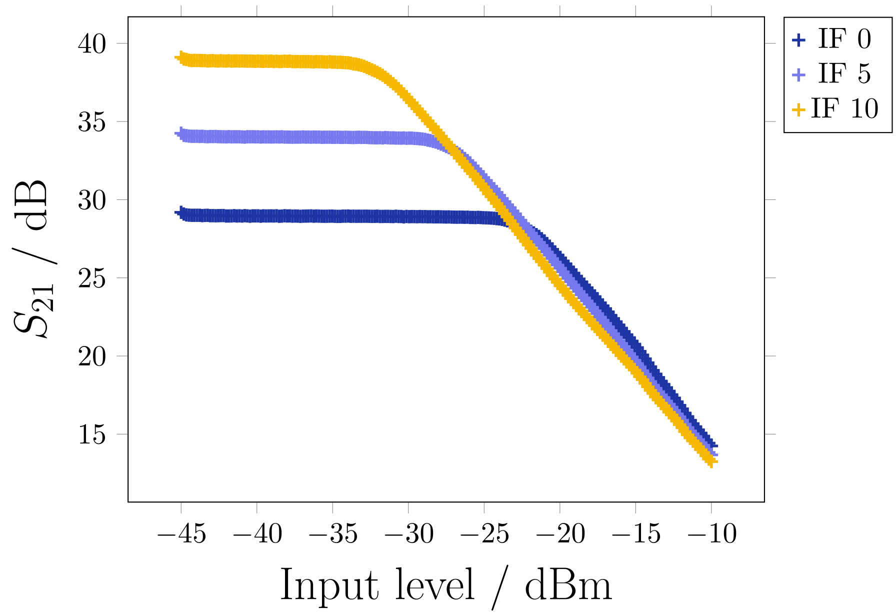

Fig. 34. S_{21} plotted against the input power to determine the 1 dB compression point of the IF amplifier.

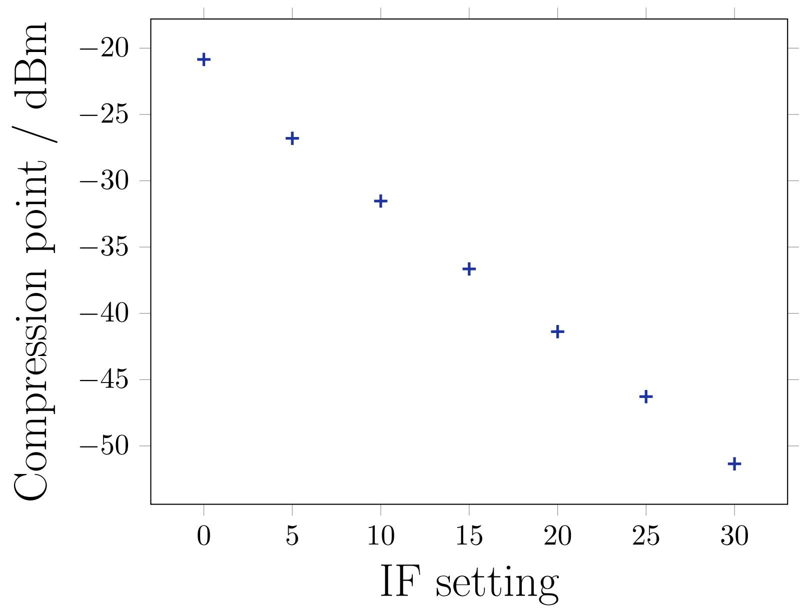

Fig. 35. S_{21} plotted against the input power to determine the 1 dB compression point of the IF amplifier.

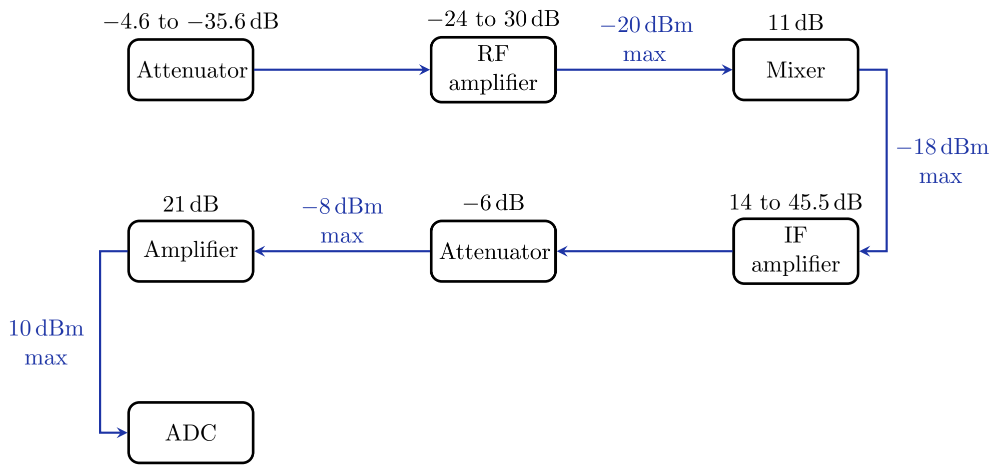

Fig. 36. The summary of the characterizations and the maximum input power for the different components.

5.6 Summary

Fig. 36 shows the components, which have to be considered, and their limitations.

Through the maximum input power of 4 dBm sent into the ADC the power sent into the amplifier behind the IF amplifier is limited to −13 dBm, which fulfills the maximum of −8 dBm. In the same way the −20 dBm limit of the IF amplifier complies with the requirements for the mixer of a maximum input power of −18 dBm. If the RF amplifier is only used to attenuate the signal if the attenuation through the attenuator is not sufficient, it also complies with the demands of the RF amplifier.

5.6.1 Software

As it is challenging to keep in mind all limitations, a software was written to count back the power sent into the board from the measured output power and the settings of the amplifiers and the attenuator and then determine good settings considering the characterizations of the different components. The goal is to have the signal as high as possible without saturating any component as this combination results into the best possible signal-to-noise ratio and with this into the best possible resolution.

At first the software determines the input power. To get correct results a setting, which ensures no component is saturated, is required. Therefore this setting has to be set manually. The further steps are undertaken by the software.

The first component, which is set by the program, is the attenuator. To meet the requirements for the IF amplifier the signal leaving the RF amplifier has to be limited to $-31\,\mathrm{dBm}$. The RF amplifier should not be used as an attenuator if the attenuation through the attenuator is sufficient. Therefore also the signal sent into the RF amplifier has to be limited to $-31\,\mathrm{dBm}$. If possible the setting for the attenuator is chosen in that way that it is just below $-31\,\mathrm{dBm}$. The setting of the RF amplifier then ensures the signal sent into the mixer has $-31\,\mathrm{dBm}$, either by further attenuating or by amplifying.

The IF amplifier is just used if the amplification of the RF amplifier is not sufficient. In Sec. 6 one can see that the IF amplifier is not necessary under current beam conditions as the signals sent by the BPM pickups are very high. Due to this the software will most of the times propose to set the IF amplifier to 0. But if the signal is very small the IF amplifier will amplify it to $-11\,\mathrm{dBm}$, which is the limit for the ADC.

The program is written in Python and the code is shown in appendix E.

6 Beam Measurements

During the time of the master thesis three measurement sessions were performed. One session in the beginning, one in the middle and one at the end. It was the goal for all sessions to find good settings and to work out the resolution of the setup.

Each measurement consists of six calibration measurements, one for each cavity and each direction, and one longer measurement consisting of 300 shots, which are analyzed using the calibration measurements. During the analysis process the correlation of the different BPMs is determined. To get the resolution the difference between the position determined by the BPM in the middle and the predicted position using the results of the two other BPMs are compared.

The analysis of the two directions is done independently. All measurements were performed with single bunched beams.

6.1 Beam Measurements November 2017

In November 2017 resolution measurements with three different DC board settings were performed. The bunch charge at the charge monitor nearest to the BPMs was 19 pC. As the beam charge monitor is some meters away from the cavity BPMs the charge is a bit lower. The best results were achieved setting the attenuator to 16, the RF amplifier to 24 and the IF amplifier to 5. With this setting the resolution in x-direction was 3.48 μm and in y-direction 2.60 μm.

Fig. 37 and 38 show the correlation between the three BPMs for the x- and y-direction. 810 is the name of the first cavity in beam direction, 820 the second and 830 the third. One can see that the points produce roughly a line. This shows that the system generally works.

The resolution is determined by comparing the position measured by the BPM 820 to the position calculated by the positions measured by BPM 810 and BPM 830. in the following it is assumed that the distance between the BPMs 810 and 820 and between the BPMs 820 and 830 are the same. Therefore the predicted position of BPM 820 is calculated by:

$$P_{820,\text{prediction}} = \frac{P_{810} + P_{830}}{2} \tag{58}$$

The correlation between the prediction and the measured position is shown in Fig. 39 for both directions. Through the plots a line is fitted. For an ideal setup these lines would have slope 1. However, different impacts like the beam tilt and the angle of the cavities in reference to the beam pipe cause a shift of the slope. To get the resolution, for each point of the plot in Fig. 39 the distance to the corresponding line is calculated. The standard deviation of these distances then yield the resolution. In Fig. 40a

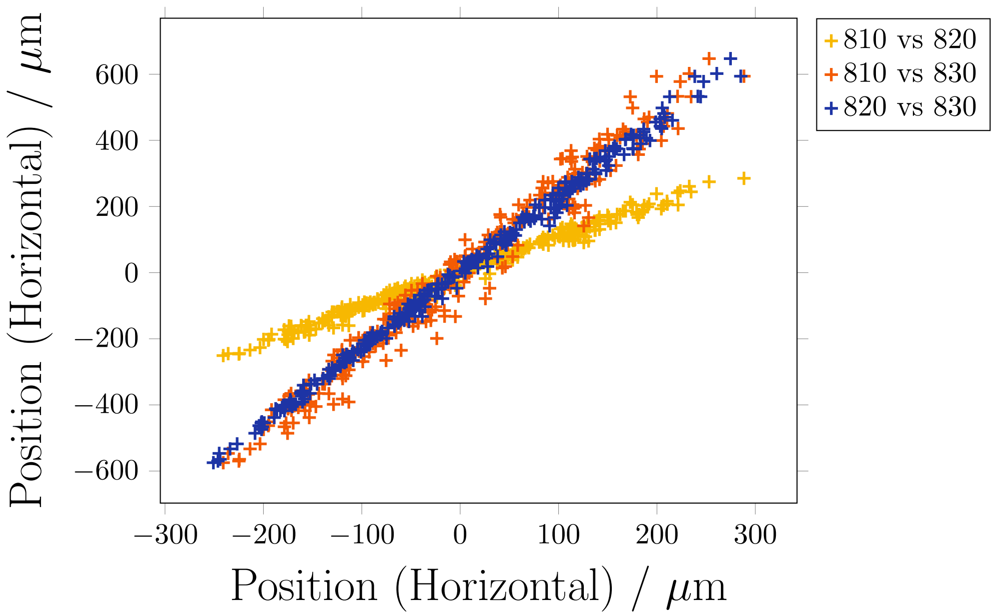

Fig. 37. Correlation of the determined horizontal positions of the three BPMs.

Settings	Resolution x / μm	Resolution y / μm
ATT 16, RF 24, IF 0	19.69	4.57
ATT 16, RF 24, IF 5	3.48	2.60
ATT 0, RF 0, IF 15	13.95	3.09

Tab. 5. Results of the resolution measurements in November 2017 and the corresponding settings of the DC board.

and 40b the histograms of the calculated distances are shown for the x- and y- direction.

The settings and the results for all performed measurements are shown in Tab. 5. The corresponding plots and the histograms are shown in appendix A.

6.2 Beam Measurements June 2018

The characterization of the DC board give that for the measurements in November an attenuation of −38.54 dB to −55.27 dB was applied by the attenuator and the amplifier. Therefore the noise figure of these measurements was very high. The goal for the measurements in June was to find better settings. To reduce the attenuation without saturating any components a reduction of the beam charge to roughly one pC was required.

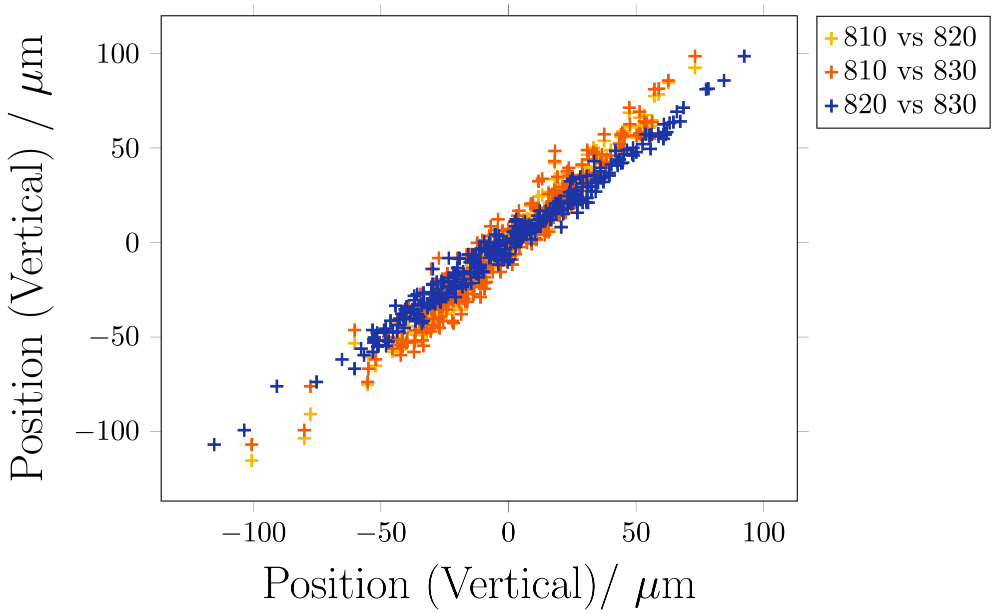

Fig. 38. Correlation of the determined vertical positions of the three BPMs.

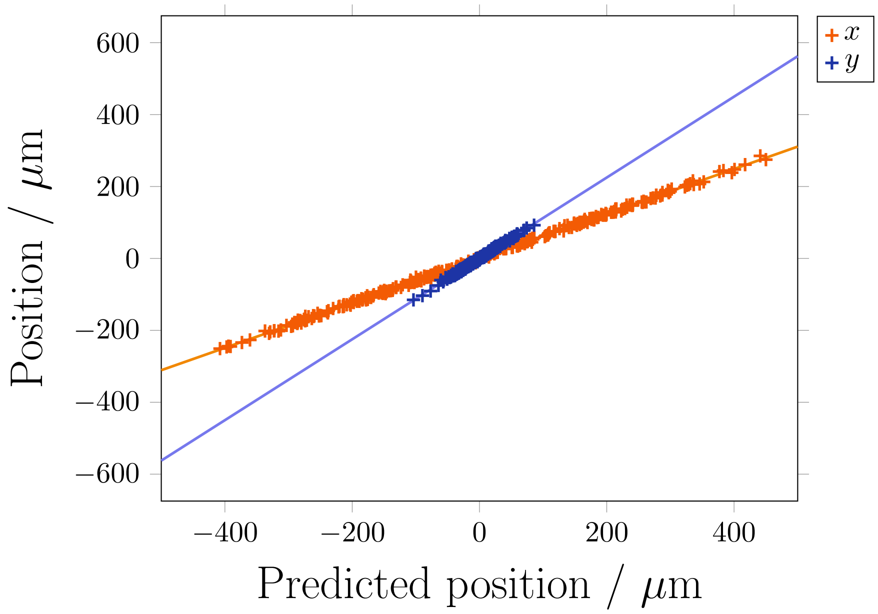

Fig. 39. Correlation of the position measured by the second BPM (820) and the position calculated using the measurements of the first (810) and the last (830) BPM. Through both plots a line is fitted. The standard deviation of the distance between the lines and the points yield the resolution.

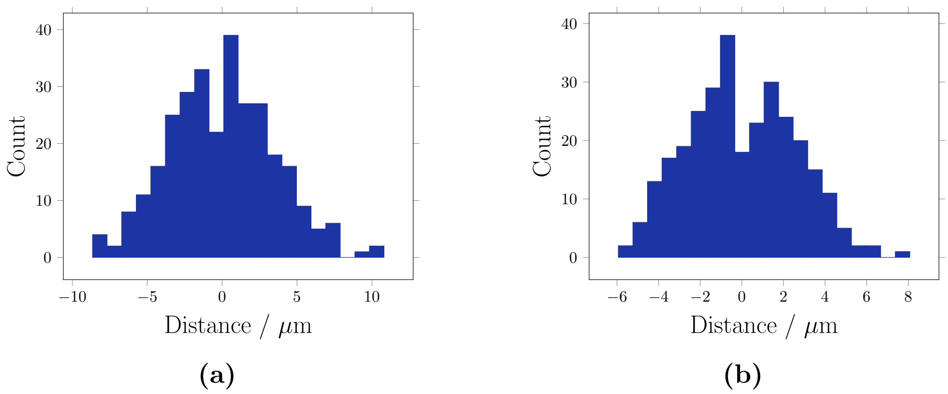

Fig. 40. Histogram of the difference between the position of the second BPM and the prediction calculated using the positions of the first and the last BPM for the x-direction (a) and the y-direction (b).

Unfortunately there was an issue with both channels of BPM 830. In Fig. 41 one can see the calibration results of the vertical channel of the BPM 830. The plots are very noisy and there is no dependency on the mover position visible. In contrast to this Fig. 41 shows the calibration results of the horizontal channel of the BPM 810. There is very little jitter and the plot of the measured position versus the position of the mover shows a staircase.

The reason for the issues is probably radiation damage on the electronics caused by an experiment with very high radiation, which was performed just before the measurements with the cavity BPMs.

However, it is possible to analyze the correlation between two BPMs assuming that there is no angular beam jitter. As the BPMs are quite far away from the beam gun, this assumption is reasonable. The analysis is performed similarly to the analysis for three BPMs. Fig. 43 shows the correlation between the two BPMs for the horizontal and the vertical plane for one out of the three performed resolution measurements. Fig. 44a and 44b show the corresponding histograms illustrating the resolution for both directions. Tab. 6 shows the determined resolution for the three performed measurements. For the beam measurements in November 2017 all DC boards were configured the same way. In June every channel was set separately. Therefore the settings are not written into the result table. For all boards the attenuator and the IF amplifier were set to 0. The RF amplifier ranges from 47 to 80.

All settings, the correlation plots and histograms for all three measurements are attached in appendix B.

Compared to the measurements in November 2017 the resolutions are worse. However, considering the beam charge they prove the great sensitivity of the pickups. The resolution is inversely proportional to the beam

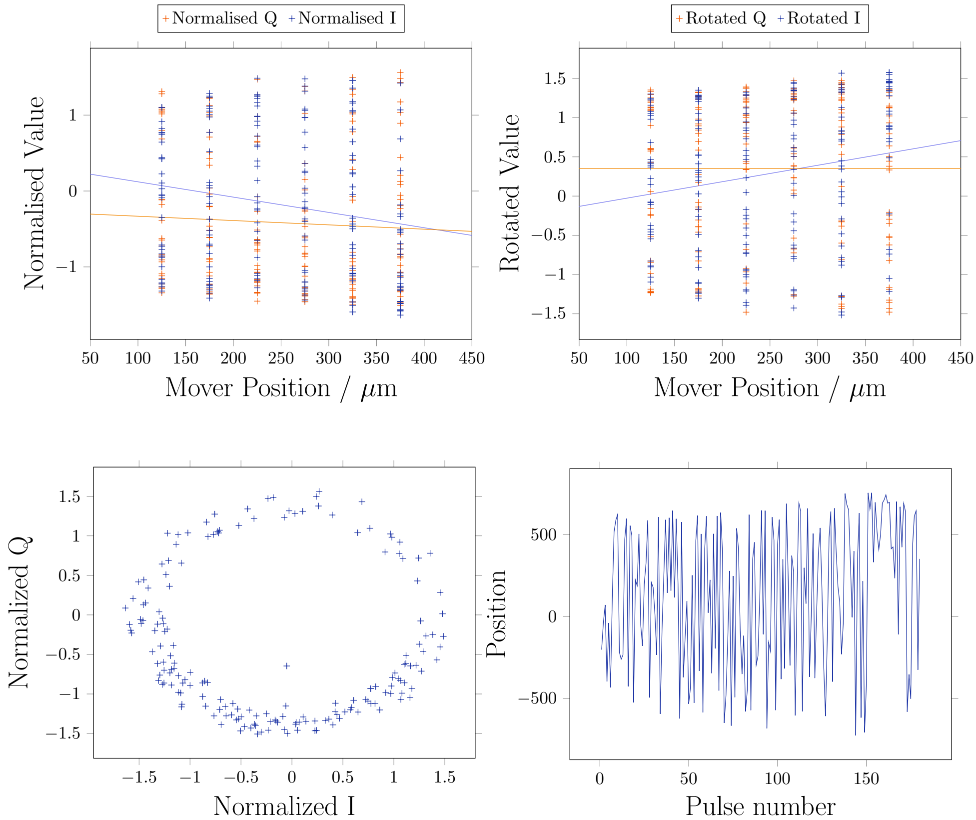

Fig. 41. Calibration results of the horizontal channel of the BPM 830. There is no dependency on the mover position visible.

Measurement	Resolution x / μm	Resolution y / μm
1	64.88	6.41
2	28.62	20.26
3	1029.60	144.69

Tab. 6. Results of the resolution measurements in June 2018.

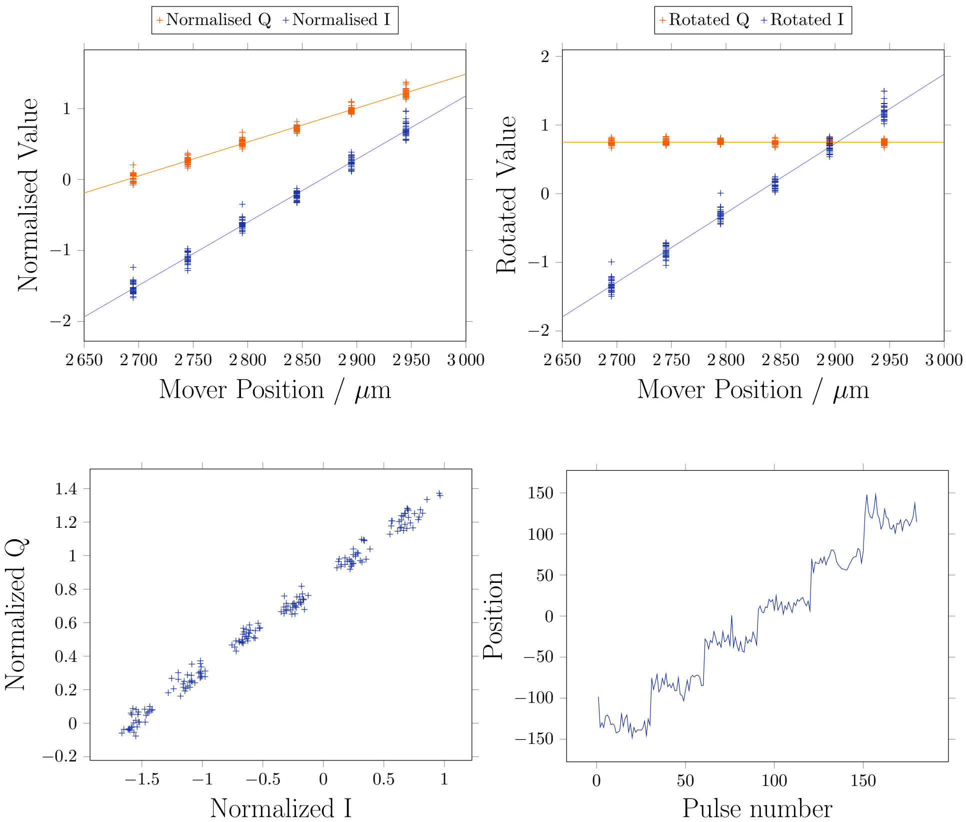

Fig. 42. Calibration results of the vertical channel of the BPM 810. The dependency of the mover position is visible very well and it is a measurement with little noise.

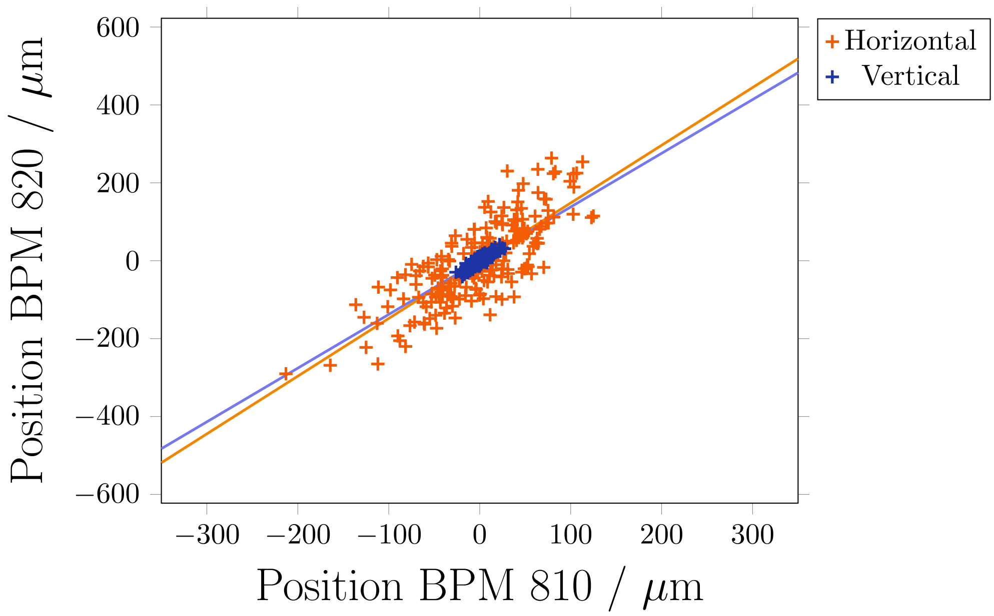

Fig. 43. Correlation between the first and the second BPM in horizontal and vertical direction. Through both plots a line is fitted.

charge [15]. CLEAR is able to produce a beam charge of 200 pC [3] and CLIC proposal [2] even specifies a bunch charge of 0.6 nC. Neglecting other limitations this would result into a possible resolution of about 30 nm for CLEAR and even about 10 nm resolution for CLIC.

6.3 Beam Measurements September 2018

After the measurement session in June, several boards were replaced to obtain three well performing BPM systems available. Unfortunately another board replacement during the measurement time was required to make all BPMs working.

The beam was single bunched with a bunch charge of 0.7 pC to decrease the applied attenuation in the board.

However when the BPM system was finally working the beam started to show an not wanted pattern. In Fig. 45 the normalized Q of the horizontal channel of the second BPM is shown. The visible cross shows that the beam switches between two different beam trajectories. One idea was that the charge is too low to run a stable beam but increasing the beam charge to 10 pC did not solve the issue. A fire alarm in the neighbour tunnel stopped further inquiries.

Despite the unstable beam conditions a resolution measurement was performed. Fig. 46 and 47 visualize the correlations between the differnet BPMs. Fig. 48 shows the comparison of the position predicted for the

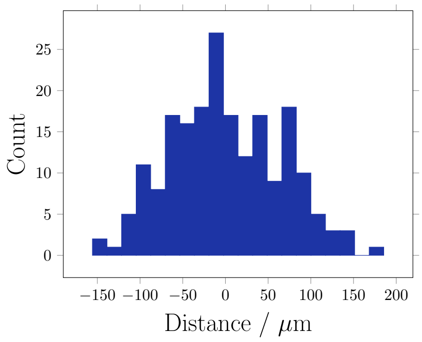

(a)

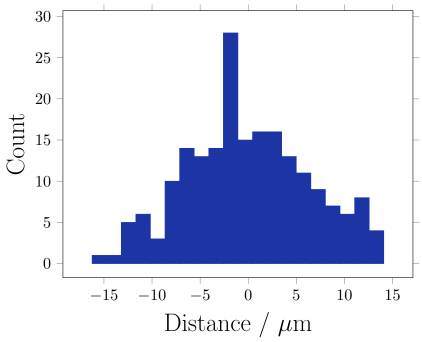

(b)

Fig. 44. Histogram of the deviation of each shot from the line fitted in the correlation plot for the horizontal direction (a) and the vertical direction (b).

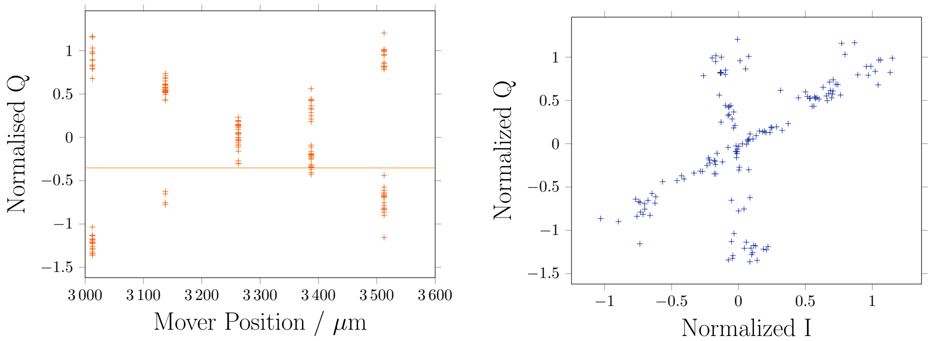

Fig. 45. Calibration results of the horizontal channel of the second BPM. A binary beam pattern is visible.

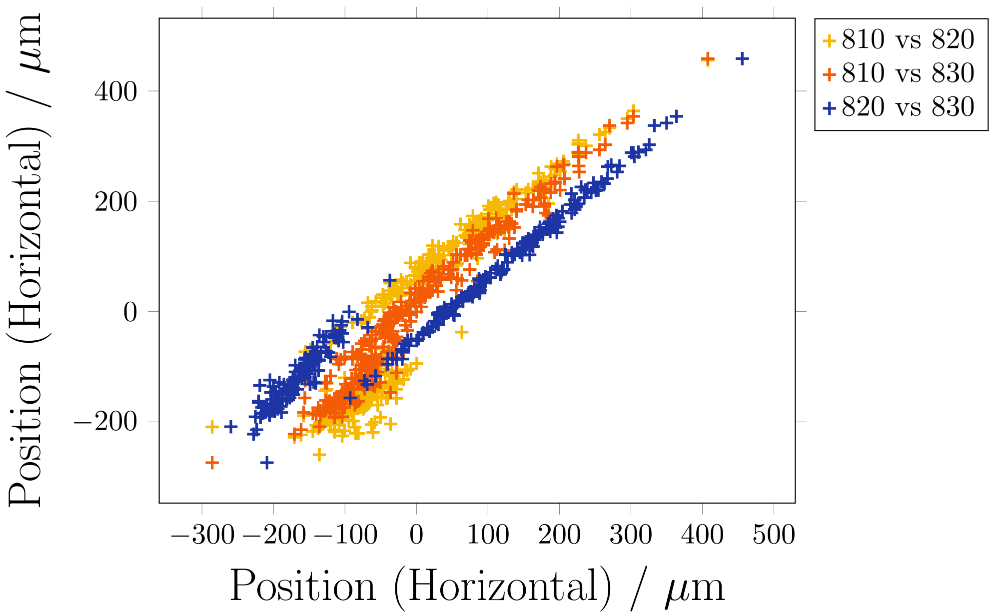

Fig. 46. Correlation of the determined horizontal positions of the three BPMs.

Measurement	Resolution x / μm	Resolution y / μm
1	96.58	20.15
2	36.62	30.60

Tab. 7. Results of the resolution measurements in September 2018.

second BPM and the measured position. Also these plots show the binary beam pattern. Tab. 7 show the determined resolutions and Fig. 49 shows a histogram of the deviation between fitted line and the measurement points of each shot.

Due to the binary beam pattern it was expected that the resolution will be worse than the resolutions determined in the measurement sessions before. But it was a further proof of the sensitivity of the bickups and also a proof that in principle all three BPM systems are able to work.

The plots, which are not in the text and the settings for all boards are shown in appendix C

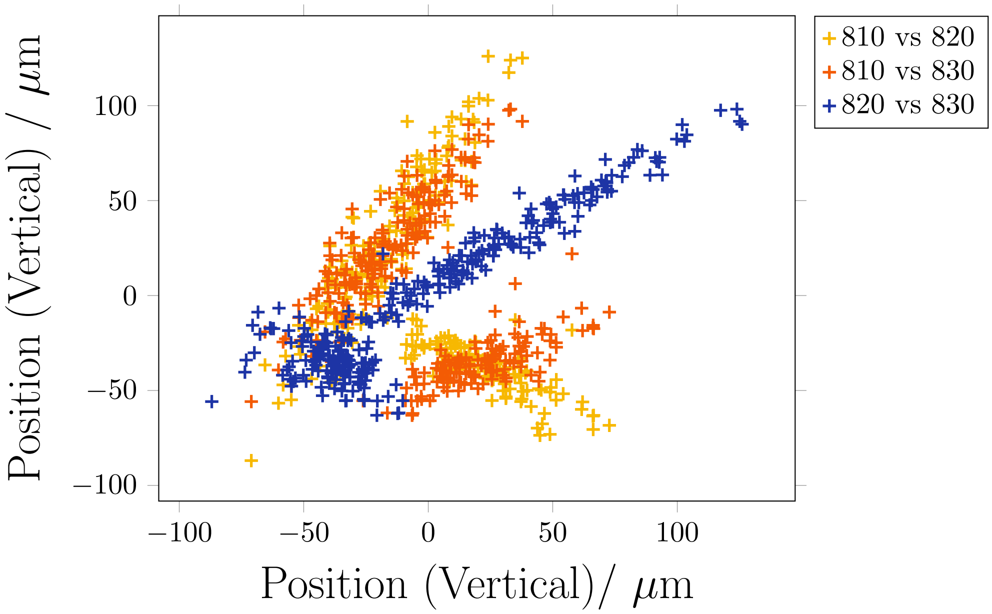

Fig. 47. Correlation of the determined vertical positions of the three BPMs.

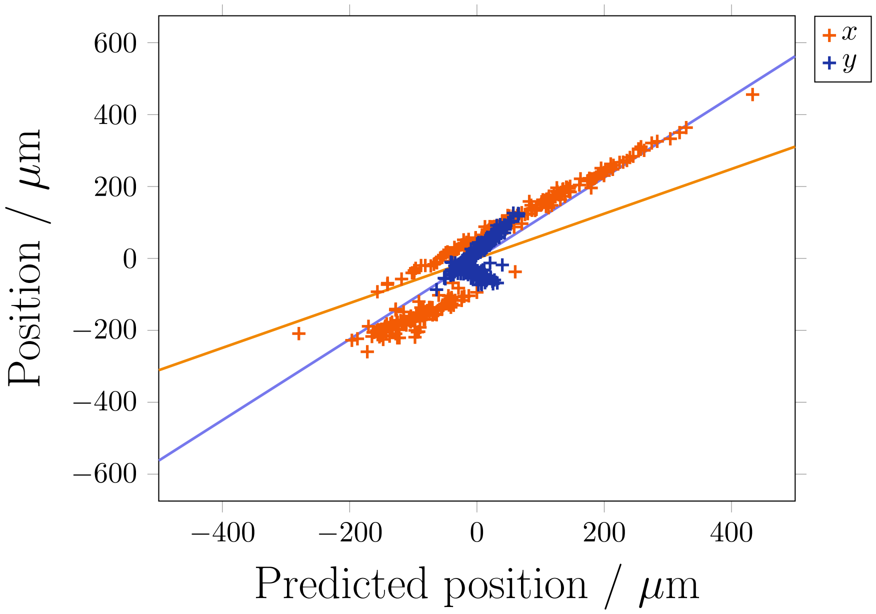

Fig. 48. Correlation of the position measured by the second BPM (820) and the position calculated using the measurements of the first (810) and the last (830) BPM. Through both plots a line is fitted. The standard deviation of the distance between the lines and the points yield the resolution.

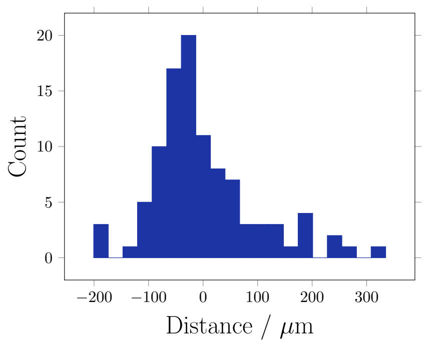

(a)

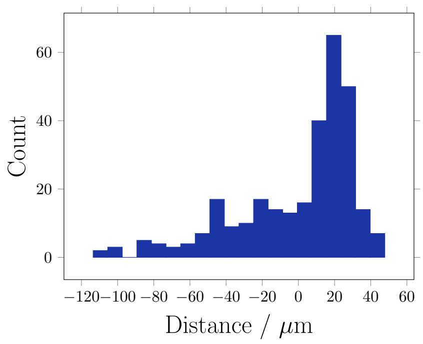

(b)

Fig. 49. Histogram of the deviation of each shot from the line fitted in the correlation plot for the horizontal direction (a) and the vertical direction (b).

7 Summary and Outlook

Two main goals have been achieved during the process of this master thesis:

- The RF front-end electronics, used for the analog signal processing and down-mixing of the 15 GHz cavity BPM signals was systematically analyzed in the laboratory. The focus of this examination was on the downconverter (DC) board, by measuring the characteristics and performance of each stage.

- Beam studies have been undertaken to understand performance and limitations of the cavity BPM system with respect to resolution and beam intensity. This included some important modifications on the control electronics and its software of the front-end electronics, which is installed in the CLEAR accelerator tunnel, thus exposed to ionising radiation.

The analysis of the DC board required an RF characterization of each stage, i.e. the RF input stage, the RF mixer, and the IF stage in terms of gain and 1 dB compression point. As RF and IF amplifiers are equipped with switched, respectively variable attenuators and gain stages, this RF analysis required more elaborate controls, which were performed by a set of Python scripts, managed through a Raspberry Pi utilized as the new DC board controller. Before this systematic study of the DC board, the observation of the beam signals was handicapped by saturation effects in the downconverter, and as it was unknown which DC stage was in overdrive, it was basically impossible to prevent the saturation without compromising a high resolution beam position measurement. Now, the results of the DC board analysis were loaded into a second Python script that determines the signal power at the RF input of the DC board from the measured signal at the IF output, and computes an optimal setting for the RF input attenuator and gain stages. For the first time, this enables a beam position measurement of the cavity BPM signal without saturation effects in the DC board, and feeding the best possible IF signal to the ADC digitizer.

Following the analysis and characterization of the DC board in the laboratory, three beam study sessions have been performed to evaluate the resolution of the present cavity BPM setup in the CLEAR accelerator.

The first beam study was scheduled at the beginning of this thesis, still with some unknown facts of the RF signal processing system. A resolution of 3.5 μm for the horizontal plane, and 2.6 μm for the vertical plane was found for a single bunch beam with a charge of approximately 20 pC. However, a later analysis of the DC boards and the cavity BPM system as a whole discovered a very unfortunate setting of the RF input attenuators, effectively damping the BPM signal by 55 dB and therefore leading to a unnecessary low signal-to-noise ratio which results in an impaired position resolution.

To demonstrate the high position resolution potential of the BPM system, a second beam measurement was performed at a later time during the thesis. Again, a single bunched beam was used, but this time with a very low charge of about 1 pC to prevent saturation effects of the RF electronics, even in case of non-optimal DC board settings. Unfortunately previous experiments performed at CLEAR damaged one of the three BPM read-out systems due to high radiation levels in the tunnel. Therefore, the resolution had to be estimated on basis of only two BPMs, which still includes beam motion effects. In this second session a horizontal resolution of 6.4 μm, and a vertical resolution of 28.6 μm was found. Evidently, the vertical measurement is dominated by beam motion, both planes should show a similar value for the resolution, as there is no fundamental difference between them. While the resolution demonstrated in this second measurement was lower compared to the first study, the resolution normalized to the bunch intensity is substantially higher, and proves the high sensitivity, i.e. the high shunt impedance of the cavity BPM. Assuming a basically linear behavior of the system, which is the case except for very small beam displacements near the BPM center, the resolution is inversely proportional to the beam charge. For a bunch charge of 0.6 nC, the proposed nominal bunch charge for CLIC, this would give a resolution in the order of 10 nm.

In the end of the thesis a third measurement session was performed. The beam charge was set to roughly 0.7 pC. Several boards had been replaced in advance to solve the issues with the third BPM. After another board change during the session this could finally be achieved. Unfortunately issues with the beam limited the achieved resolution to 20.15 μm in the horizontal and 36.62 μm in the vertical direction but it could be shown that the setup is prepared for another measurement with a stable beam.

Summarizing the results and experience from both beam studies, and including the characterization of the RF front-end electronics in the laboratory, a few conclusion can be made:

- The cavity BPM pickups have a very high resolution potential, probably even better than 50 nm, and meet the requirements as specified in the CLIC design report.
- The RF frontend electronics fulfills some of the basic requirements, but has shortcomings in terms of radiation tolerance and being very fragile in the handling.
- The shot-to-shot beam jitter at CLEAR is rather high, typically some or even many μm, while the gain of the RF electronics is very high. This combination caused major trouble and calls for redesign and simplification of the RF front-end.

Following those conclusions, a simple passive downconverter based on radiation tolerant components located close to the cavity BPM pickups in the tunnel, followed by an active IF section outside the tunnel seems to be a good compromise to match the operational beam conditions of CLEAR with a reliable, high resolution read-out system.

The introduction of the Raspberry Pi with Python scripts as controller for the RF electronics was a quick, flexible, low cost solution, and demonstrated to be a key component for the success of this study and this thesis. A different, more "professional" GPIO control board, e.g VME-based, might have some advantages, however, for the time being we will continue to use the Raspberry Pi solution.

In summary, the results of this thesis define the next steps of the project, particular to derive the specifications for a revised, and simplified RF front-end electronics. The beam measurements demonstrated, the cavity BPM pickups already meet the specification for a resolution of 50 nm, or better. An easy-to-use GUI for the BPM operation in the control room does not exist yet, but the Python scripts written during this thesis can constitute as a helpful debugging tool.

A Appendix for Beam Measurements in November

A.1 Plots for ATT 0, RF 0, IF 5

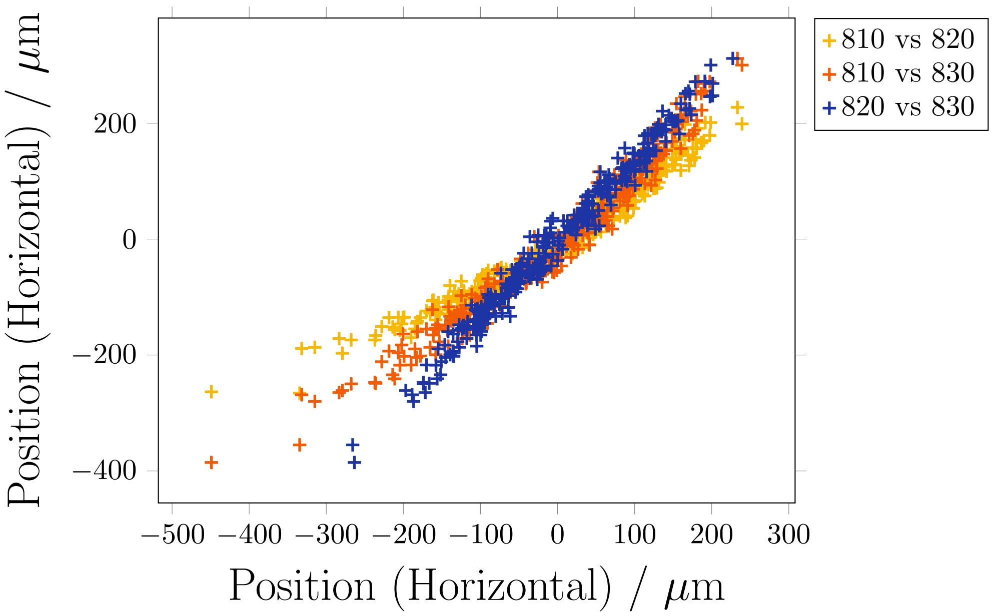

Fig. 50. Correlation of the determined horizontal positions of the three BPMs.

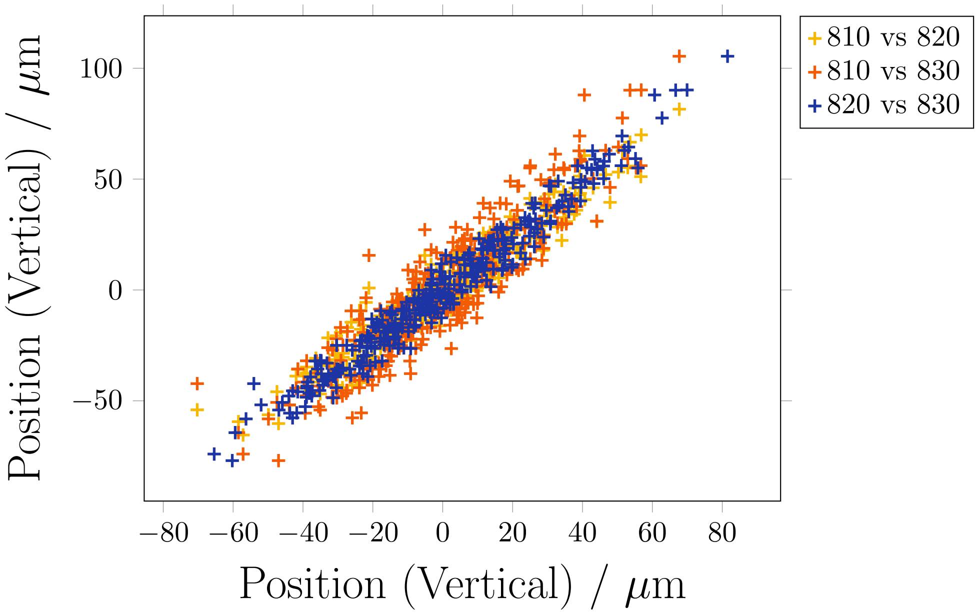

Fig. 51. Correlation of the determined vertical positions of the three BPMs.

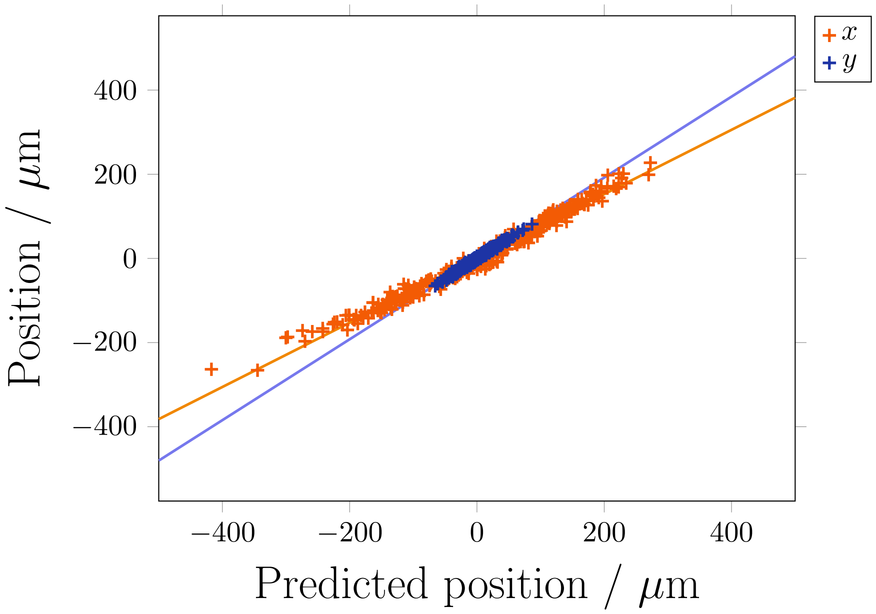

Fig. 52. Correlation of the position measured by the second BPM (820) and the position calculated using the measurements of the first (810) and the last (830) BPM. Through both plots a line is fitted to. The standard deviation of the distance between the lines and the points yield the resolution.

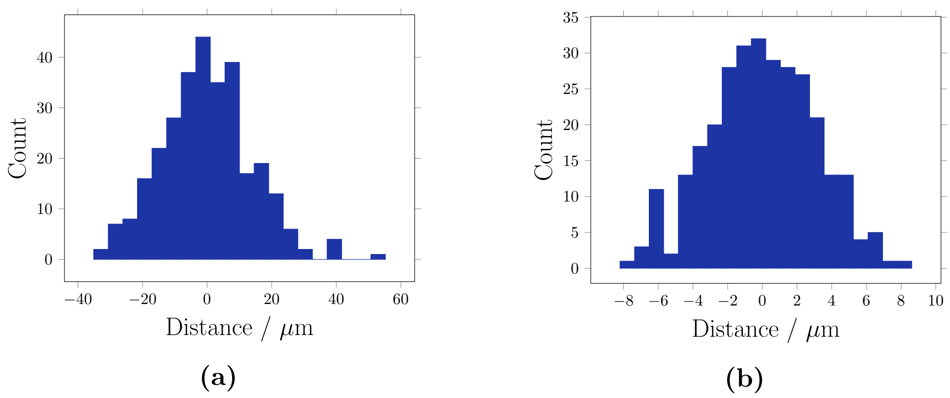

Fig. 53. Histogram of the difference between the position of the second BPM and the prediction calculated using the positions of the first and the last BPM for the x-direction (a) and the y-direction (b).

A.2 Plots for ATT 16, RF 24, IF 5

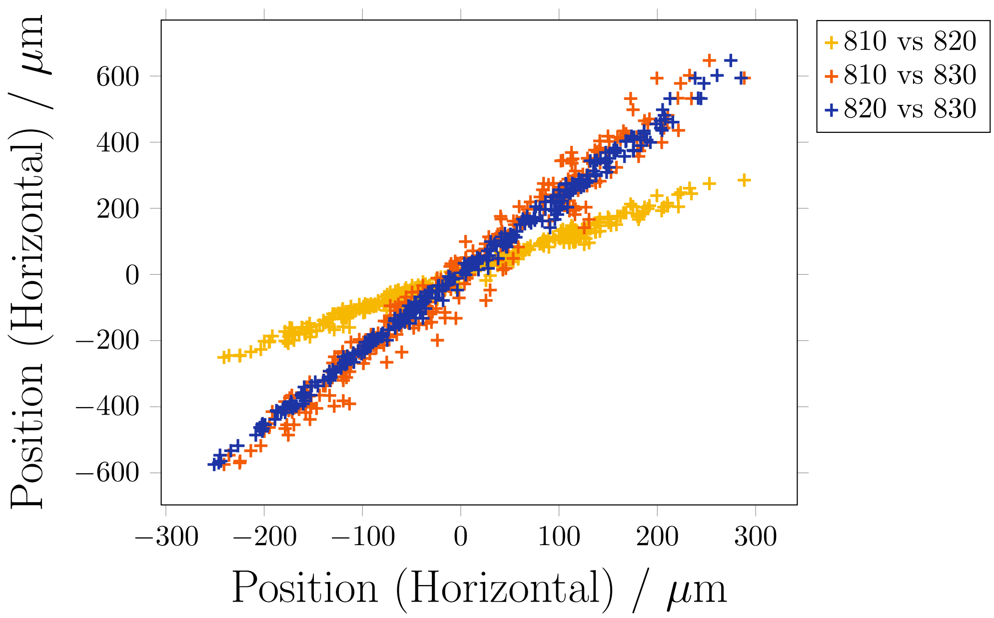

Fig. 54. Correlation of the determined horizontal positions of the three BPMs.

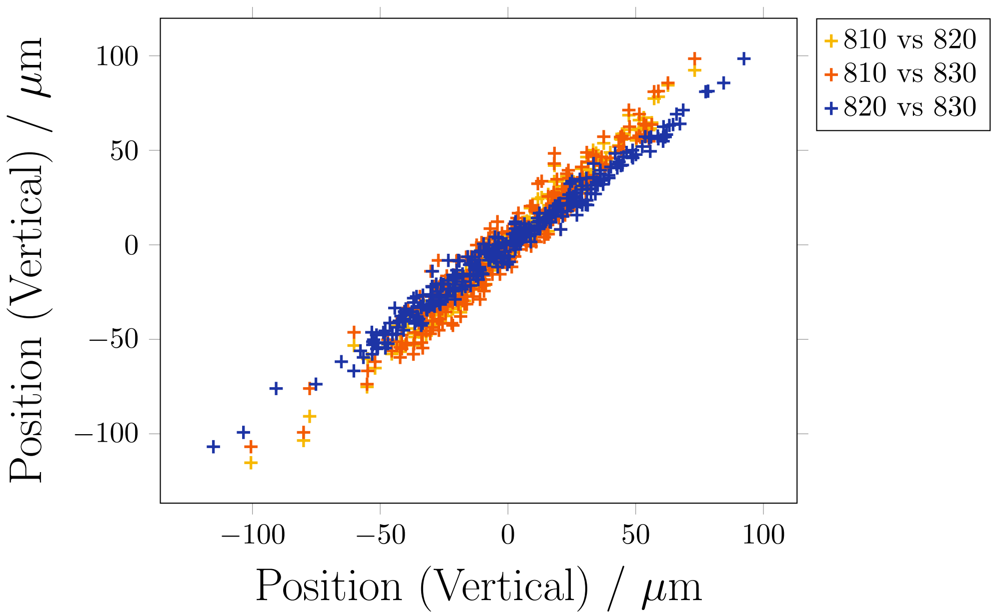

Fig. 55. Correlation of the determined vertical positions of the three BPMs.

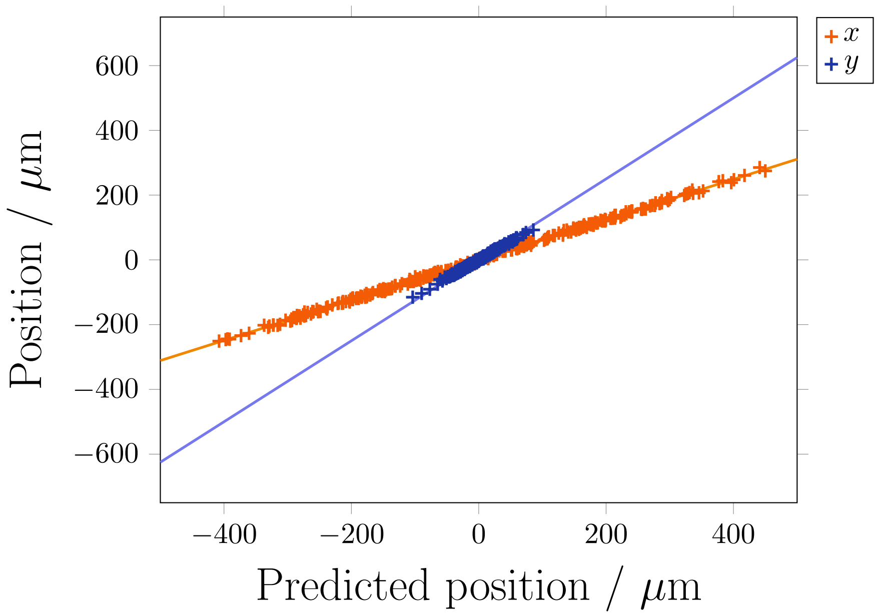

Fig. 56. Correlation of the position measured by the second BPM (820) and the position calculated using the measurements of the first (810) and the last (830) BPM. Through both plots a line is fitted to. The standard deviation of the distance between the lines and the points yield the resolution.

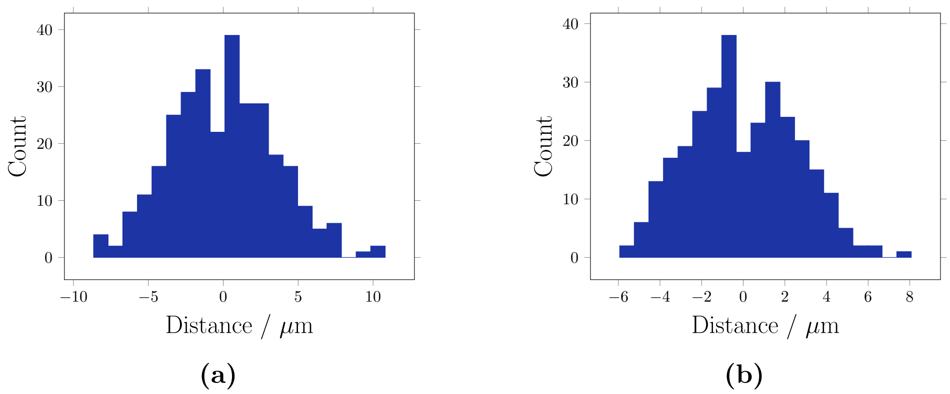

Fig. 57. Histogram of the difference between the position of the second BPM and the prediction calculated using the positions of the first and the last BPM for the x-direction (a) and the y-direction (b).

B Appendix for Beam Measurements in June

B.1 Settings for Measurement 1

Channel	**Attenuator**	**RF Amplifier**	**IF Amplifier**
810M	0	57	0
810H	0	72	0
820H	0	56	0
830H	0	47	0
810V	0	70	0
820V	0	80	0
830V	0	60	0

Tab. 8. Settings for all channels for beam measurement 1 in June.

B.2 Plots and Settings for Measurement 2

Channel	**Attenuator**	**RF Amplifier**	**IF Amplifier**
810M	0	57	0
810H	0	57	0
820H	0	50	0
830H	0	47	0
810V	0	70	0
820V	0	80	0
830V	0	47	0

Tab. 9. Settings for all channels for beam measurement 2 in June.

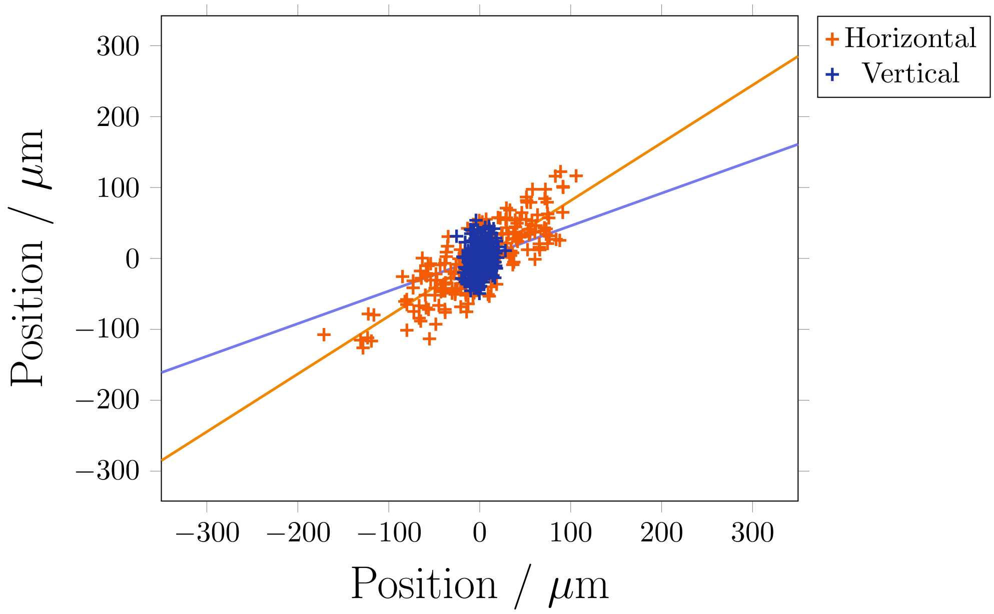

Fig. 58. Correlation and fit of the determined horizontal positions of the three BPMs.

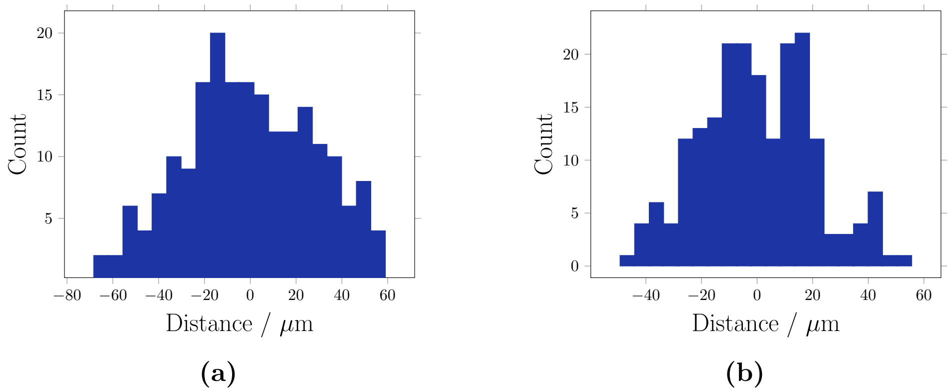

Fig. 59. Histogram of the deviation of each shot from the line fitted in the correlation plot for the x-direction (a) and the y-direction (b).

B.3 Plots and Settings for Measurement 3

Channel	Attenuator	RF Amplifier	IF Amplifier
810M	0	57	0
810H	0	47	0
820H	0	50	0
830H	0	47	0
810V	0	70	0
820V	0	80	0
830V	0	47	0

Tab. 10. Settings for all channels for beam measurement 3 in June.

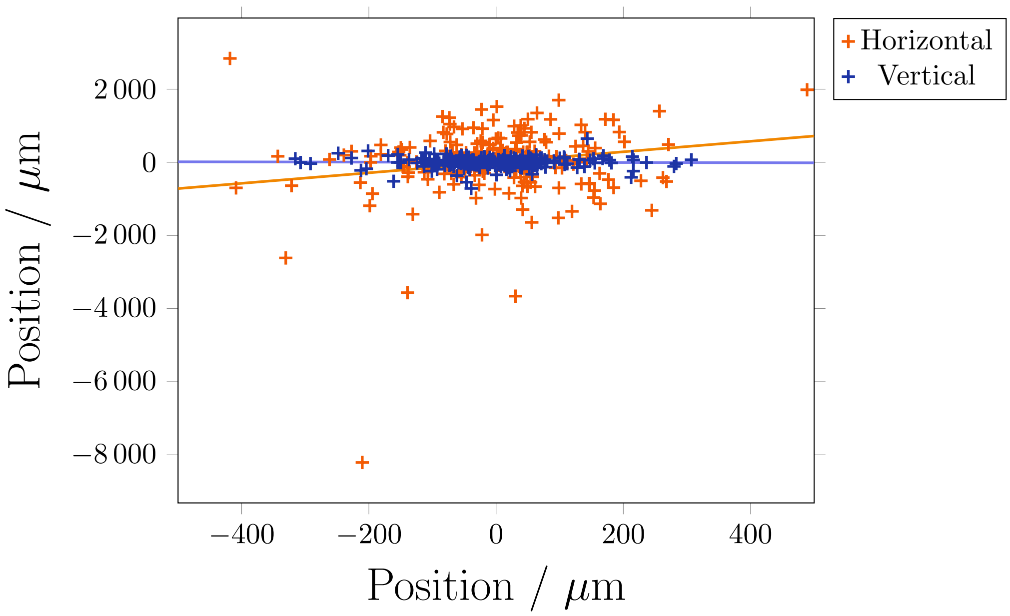

Fig. 60. Correlation and fit of the determined horizontal positions of the three BPMs.

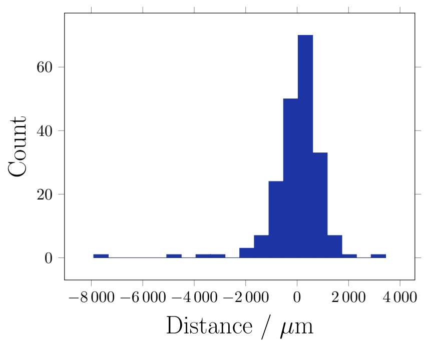

(a)

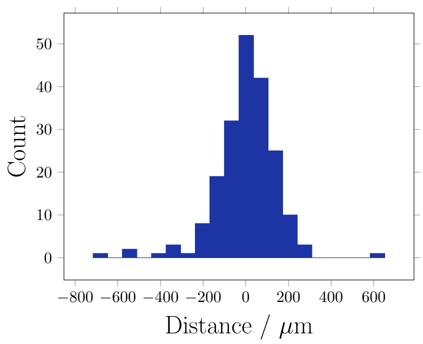

(b)

Fig. 61. Histogram of the deviation of each shot from the line fitted in the correlation plot for the x-direction (a) and the y-direction (b).

C Appendix for Beam Measurements in September

C.1 Settings of all channels for both measurements

Channel	Attenuator	RF Amplifier	IF Amplifier
810H	14	48	0
820H	10	48	0
830H	0	48	0
810V	0	48	0
820V	10	48	0
830V	0	47	0

Tab. 11. Settings for all channels for the measurements in September.

C.2 Plots for Measurment session 1

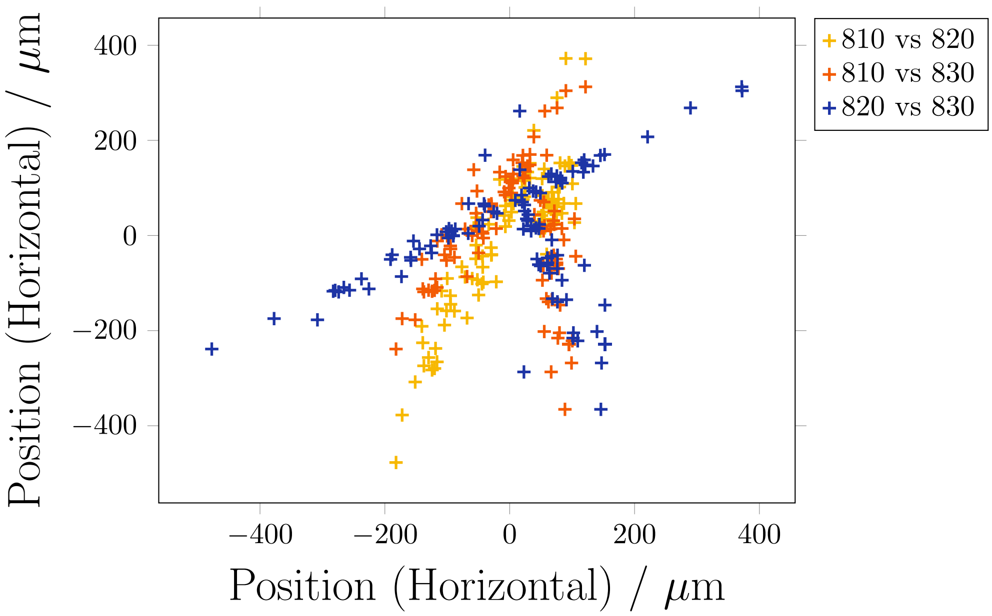

Fig. 62. Correlation of the determined horizontal positions of the three BPMs.

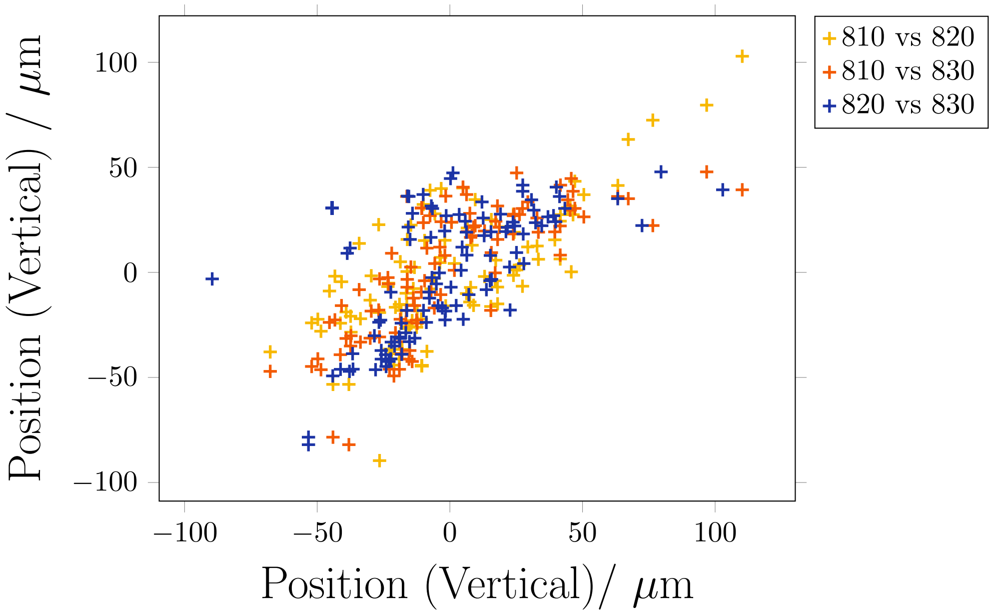

Fig. 63. Correlation of the determined vertical positions of the three BPMs.

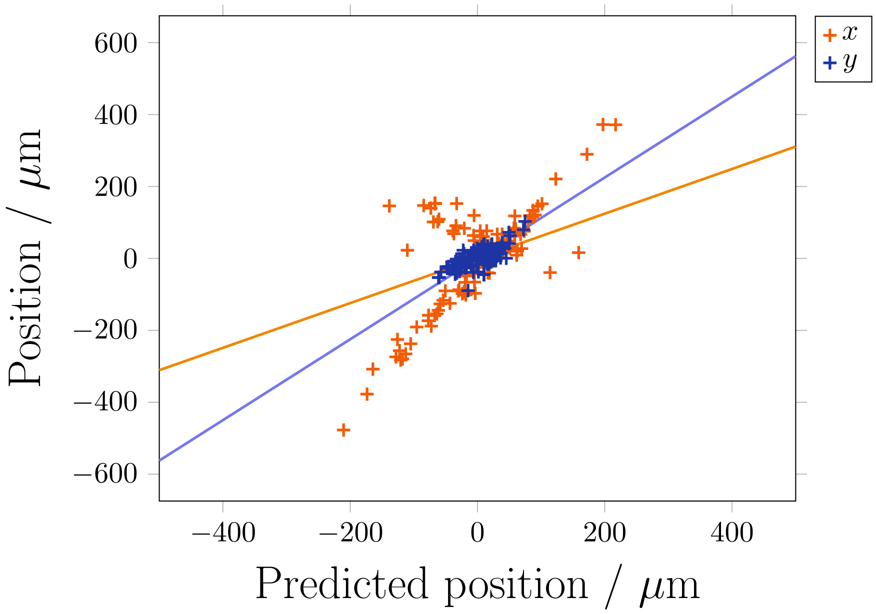

Fig. 64. Correlation of the position measured by the second BPM (820) and the position calculated using the measurements of the first (810) and the last (830) BPM. Through both plots a line is fitted. The standard deviation of the distance between the lines and the points yield the resolution.

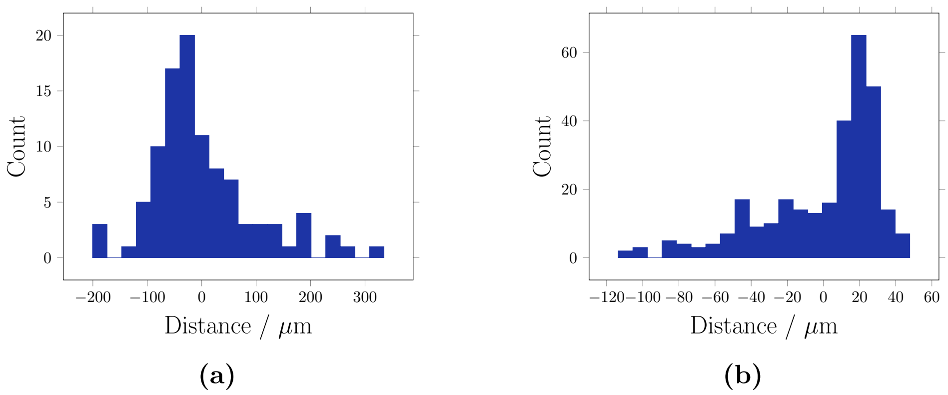

Fig. 65. Histogram of the deviation of each shot from the line fitted in the correlation plot for the horizontal direction (a) and the vertical direction (b).

D Software for Automated Characterization

```
from instrument import Instrument
import cbpmControl_2B
import time
import usbtmc
import matplotlib.pyplot as plt
import csv

attenuationCable=1.16
attenuationBoard=4.60
attenuationSplitter=20


class Instrument:

    def __init__ (self):
        self.callname = usbtmc.Instrument(0x0b5b, 0
           x0006)
        self.name = self.query('*IDN?')
        print (self.name, " has been initialized")


    def initializeDevice (self):
        self.selfTest()
        self.reset()
        self.setLanguageNative()
        self.loadApplication()


    def closeConnection (self):
        self.callname.close()


    def loadApplication (self):
        print ("Waiting for the device to load
           application ...")
        self.callname.write("MMEM:LOAD:STAT '
           Param20180404_023'")
        time.sleep(60) #Yes, it needs so long
```

```
    def measureAmplitude (self):
        self.callname.write('SYST:LANG SCPI;*WAI')
        self.callname.write('CALC:MARK:MAX')
        self.setLanguageNative()
        self.callname.write('SYS SPECT')
        self.callname.write('INIT:MODE:CONT')
        amplitude = self.callname.ask('MKL?')
        return amplitude


    def reset (self):
        print ("Waiting for the device to reset
           ...")
        self.callname.write('*RST')
        time.sleep(30) # Yes, it needs so long


    def selfTest (self):
        status = self.query('*TST?')
        if status == '0':
            print ("Instrument passed selftest")
        else:
            print ("Instrument failed selftest")


    def setLanguageNative (self):
        self.callname.write('SYSTem:LANGuage NATive
           ;*WAI')


    def setLanguageSCPI (self):
        self.callname.write('SYST:LANG SCPI;*WAI')


    def query (self, visaString):
         return self.callname.ask (visaString)


def expertMode (serialnumber, address):
    component = getValidComponent ()
    maximum = getMaxConfiguration(component)
    start = getValidStart (maximum)
    end = getValidEnd (start, maximum)
    stepwidth = getValidStepwidth (start, end)
```

```
    performMeasurement(serialnumber, address, level,
        component, start, end, stepwidth)


def getMaxConfiguration (component):

    if component == 'rf':
        maxConfiguration = 255
    else:
        maxConfiguration = 31
    return maxConfiguration


def getValidAddress ():

    invalidInput = True
    while invalidInput == True:
        address = int(input("Enter the address of
           the board: "))
        if address in range(0,16):
            invalidInput = False
        else:
            print("Sorry, this adress doesn't exist
               .")
    return address


def getValidComponent ():

    invalidInput = True
    while invalidInput == True:
        component = raw_input ("Which component
           shall be tuned (rf, if, att)? ")
        if component in ('att', 'rf', 'if'):
            invalidInput = False
        else:
            print ("Sorry, this is not a valid
               component")
    return component


def getValidSerialnumber ():

    invalidInput = True
```

```
    while invalidInput == True:
        serialnumber = int(input("Enter the serial
           number of the board: "))
        if serialnumber in range(1,15):
            invalidInput = False
        else:
            print("Sorry, this serialnumber doesn't
               exist.")
    return serialnumber


def getValidEnd (start, maximum):

    invalidInput = True
    while invalidInput == True:
        end = int(input("Enter the end point (
           Integer): "))
        if end in range(start, maximum):
            invalidInput = False
        else:
            print("Sorry, this end point is smaller
               than the start or larger than the
               maximum.")

    return end


def getValidRfGain ():

    invalidInput = True
    while invalidInput == True:
        rfGain = int(input("Enter a valid RF gain ")
           )
        if rfGain in range(0,256):
            invalidInput = False
        else:
            print("Sorry, RF gain is out of range.")
    return rfGain


def getValidStart(maximum):

    invalidInput = True
    while invalidInput == True:
```

```
        start = int(input("Enter the start point (
           Integer): "))
        if start in range(0,maximum+1):
            invalidInput = False
        else:
            print("Sorry, start point is out of
               range.")
    return start


def getValidStepwidth (start, end):

    invalidInput = True
    while invalidInput == True:
        stepwidth = int(input("Enter the stepwidth (
           Integer): "))
        if stepwidth < end-start:
            invalidInput = False
        else:
            print("Sorry, Stepwidth is too large.")

    return stepwidth


def performMeasurement (serialnumber, address, level
   , component, start, end, stepwidth):

    signalAnalyzer = Instrument()

    if component == 'rf':
        function = cbpmControl_2B.setRF
        timestamp = time.strftime("%Y%m%d%H%M", time
           .localtime())
        filename="gainMeasurement_board" + str(
           serialnumber) +"_"+ component+ "_level"+
           str(level) +"_"+ str(timestamp)
    elif component == 'if':
        function = cbpmControl_2B.setIF
        rfGain = getValidRfGain()
        timestamp = time.strftime("%Y%m%d%H%M", time
           .localtime())
        filename="gainMeasurement_board" + str(
           serialnumber) +"_"+ component+ "_level"+
           str(level) +"_rf"+str(rfGain)+"_"+ str(
```

```
            timestamp)
    elif component == 'att':
        function = cbpmControl_2B.setATT
        timestamp = time.strftime("%Y%m%d%H%M", time
            .localtime())
        filename="gainMeasurement_board" + str(
            serialnumber) +"_"+ component+ "_level"+
            str(level) +"_"+ str(timestamp)
    else:
        print "something went wrong setting the
            right cbpmControl functions"

    trueLevel = float(level)-attenuationCable
    setGain = []
    measuredGain = []
    for index in range(start, end+1, stepwidth):
        print "new setting: ", index, " dB"
        function(address, index)
        time.sleep(7)
        measuredAmplitude = float(signalAnalyzer.
            measureAmplitude())
        trueAmplitude = float(measuredAmplitude)+
            attenuationCable+attenuationSplitter+
            attenuationBoard
        gain = trueAmplitude-trueLevel
        print gain
        setGain.append(index)
        measuredGain.append(gain)

    produceAndSavePlot(filename, setGain,
        measuredGain)
    saveRawData(filename, setGain, measuredGain)
    print filename


def produceAndSavePlot(filename, setGain,
    measuredGain):

    fig=plt.figure()
    plt.scatter(setGain, measuredGain)
    plt.ylabel('Measured Gain in dB')
    plt.xlabel('Set Value')
    plt.show()
    fig.savefig("data/gainMeasurements/"+filename+".
```

```
        pdf")


def saveRawData(filename, setGain, measuredGain):

    with open('data/gainMeasurements/' + filename +
        '.csv', 'w') as file:
         writer = csv.writer(file, delimiter='\t')
         writer.writerows(zip(setGain,measuredGain))



def runMeasurement ():
    serialnumber = getValidSerialnumber()
    address = getValidAddress ()
    level = input("Enter the Level tuned at the
        signal generator")

    print ("Choose one of the following measuring
        configurations (Format: component, start, end
        , stepwidth")
    print ("rf = RF amplifier, att = RF attenuator,
        if = IF amplifier")
    print ("0: \t Experts mode (Choose everything)")
    print ("1: \t rf, 0, 255, 1")
    print ("2: \t rf, 0, 255, 32")
    print ("3: \t if, 0, 31, 1")
    print ("4: \t if, 0, 31, 4")
    print ("5: \t att, 0, 31, 1")
    print ("6: \t att, 0, 31, 4")
    numberConfiguration = int(input ("Choose a
        number! "))

    if numberConfiguration == 0:
         expertMode(serialnumber, address)

    elif numberConfiguration == 1:
         performMeasurement(serialnumber, address,
            level, 'rf', 0, 255, 1)

    elif numberConfiguration == 2:
         performMeasurement(serialnumber, address,
            level, 'rf', 0, 255, 32)

    elif numberConfiguration == 3:
```

```
        performMeasurement(serialnumber, address,
           level, 'if', 0, 31, 1)

    elif numberConfiguration == 4:
        performMeasurement(serialnumber, address,
           level, 'if', 0, 31, 4)

    elif numberConfiguration == 5:
        performMeasurement(serialnumber, address,
           level, 'att', 0, 31, 1)

    elif numberConfiguration == 6:
        performMeasurement(serialnumber, address,
           level, 'att', 0, 31, 4)

    else:
        print ("Something in the Configuration
           process went wrong")


def checkLookuptable(boardSerialnumber, boardAddress
   , level):

    setGain = []
    measuredGain = []
    signalAnalyzer = Instrument()
    trueLevel = float(level)-attenuationCable
    possibleSettings, possibleGains = readFile(
       configurationFileRfAmplifier)

    for k in range(34,91):
        setGain.append(possibleGains[k])
        setRF(boardAddress, possibleSettings[k])
        time.sleep(7)
        measuredAmplitude = float(signalAnalyzer.
           measureAmplitude())
        print measuredAmplitude
        trueAmplitude = float(measuredAmplitude)+
           attenuationCable+attenuationSplitter+
           attenuationBoard
        gain = trueAmplitude-trueLevel
        measuredGain.append(gain)

    filename = "checkLookuptable_board" + str(
```

```
   boardSerialnumber) + "level_" +str(level)
produceAndSavePlot(filename, setGain,
   measuredGain)
saveRawData(filename, setGain, measuredGain)
```

E Software to Determine the Best Settings

```
from dataFile import *
import csv
import numpy as np


def getBestSettings(inputPower):

    bestAtt = findAttSetting (inputPower)

    powerInRf = inputPower + setAtt_2_amplification
       (bestAtt)
    bestRf = findRfSetting (powerInRf)

    powerInIf = powerInRf + setRf_2_amplification (
       bestRf) + mixer_amplification
    bestIf = findIfSetting (powerInIf)

    print("Best Att setting: ", bestAtt)
    print("Best RF setting: ", bestRf)
    print("Best IF setting: ", bestIf)

    if (bestRf==34 and bestIf==0):
        print("The signal power is very high. Danger
            of Saturation though full attenuation.")


def getPowerIn (powerOutVoltP, setAtt, setRf, setIf)
   :

    powerOut = 10*np.log10((powerOutVoltP*2)
       **2/(0.008*50))
    print (powerOut)

    if_amplification = setIf_2_amplification (setIf)
    rf_amplification = setRf_2_amplification (setRf)
    att_amplification = setAtt_2_amplification (
       setAtt)

    powerIn=powerOut - if_amplification
    print("At IF MON", powerIn)
    powerIn=powerIn - mixer_amplification
```

```
    print ("At RF MON", powerIn)
    powerIn = powerIn - rf_amplification - float(
       att_amplification)

    return powerIn


def findAttSetting (inputPower):

    for i in range(0,32):
        powerInRf = inputPower +
           setAtt_2_amplification(i)
        bestAtt = i
        if (powerInRf <= -31):
            break

    return bestAtt


def findIfSetting (powerInIf):

    for i in np.arange(31,-1,-1):
        powerOut = powerInIf + setIf_2_amplification
           (i)
        bestIf = i
        if (powerOut <= 10):
            break

    return bestIf


def findRfSetting (powerInRf):

    for i in np.arange(91,33,-1):
        powerInMixer = powerInRf +
           setRf_2_amplification(i)
        bestRf = i
        if (powerInMixer <= -31):
            break

    return bestRf


def readFile(filename):
```

```
    invalidInput = True
    with open(filename, 'r') as file:
        reader = csv.reader(file, delimiter='\t')
        array = list(reader)

    setGain, measuredGain = zip(*array)
    setGain = map(int, setGain)
    measuredGain = [float(i) for i in measuredGain]
    return setGain, measuredGain


def setAtt_2_amplification(setAtt):

    att_amplification = setAtt * att_slope +
       att_offset
    return att_amplification


def setIf_2_amplification (setIf):

    if_amplification = setIf * if_slope + if_offset
    return if_amplification


def setRf_2_amplification (setRf):

    setting_lookup, amplification_lookup = readFile(
       filename_rf_amplification)
    rf_amplification = amplification_lookup[setRf]

    return rf_amplification
```

Acknowledgements

I owe thanks to a may people, who supported this master thesis. At first I want to thank my Supervisor in Germany Jörg Pretz for providing me a lot of free space and help, whenever it was necessary. Then I want to thank my Supervisor at CERN Manfred Wendt and Alexey Lyapin from RHUL for guyding and supporting my way into electroncis and for proof readings. I also owe a big thanks to Prof. Achim Stahl. He connected all people involved and made it possible for me to spend this great year at CERN. A great thanks goes to the research center Jülich and the research center CERN for funding the thesis and provding support for all formalities. I also want to thank the CLEAR team, especially Kyrre Sjobaek, for helping in the tunnel and providing the possibility to perform beam measurements. And I owe thanks to my familiy for proof readings and general support. And finally I want to say a special thanks to my section at CERN for an awesome working environment including a lot of scientific help but also many coffee breaks and free time activities.

References

[1] Welcome to the compact linear collider website. http://clic-study.web.cern.ch/. (Visited: 7/5/2018).

[2] Clic parameter list 3 tev. https://clic-meeting.web.cern.ch/clic-meeting/clictable2010.html. (Visited: 7/5/2018).

[3] Beam line description. https://clear.web.cern.ch/content/beam-line-description. (Visited: 7/5/2018).

[4] D. Adey et al. nustorm - neutrinos from stored muons: Proposal to the fermilab pac. FERMILAB-PROPOSAL-1028arXiv:1308.6822.

[5] Peter Forck, Piotr Kowina, and Dimitry Liakin. Beam position monitors. http://apps.fz-juelich.de/pax/paxwiki/images/2/2c/Cas_bpm_main.pdf. (Accessed 16.10.2017).

[6] University Bonn ELSA facility. Hohlraumresonatoren/ cavities. http://www-elsa.physik.uni-bonn.de/Lehrveranstaltungen/FP-E106/E106-Erlaeuterung en.pdf. (Accessed 26.10.2017).

[7] Francis Cullinan. *Development of a Prototype Cavity Beam Position Monitor for the Compact Linear Collider*. PhD thesis, Royal Holloway, University of London, 2014.

[8] N. Chritin, H. Schmickler, L. Soby, A. Lunin, N. Solyak, M. Wendt, and V. Yakovlev. A high resolution cavity bpm for the clic test facility. In *Beam instrumentation. Proceedings, 14th Workshop, BIW10, Santa Fe, USA, May 2-6, 2010*, 2010.

[9] Jack R Towler, Stewart Boogert, Brian Fellenz, Thibaut Lefévre, Alexey Lyapin, and Manfred Wendt. Development and Test of High Resolution Cavity BPMs for the CLIC Main Beam Linac. page TUPB060. 5 p, 2016.

[10] TriQuint Semiconductor Inc. Tgm2543-sm. https://www.qorvo.com/products/d/da005048. (Accessed 13.08.2018).

[11] Analog Devices Inc. Hmc939. http://www.analog.com/media/en/technical-documentation/data-sheets/hmc939chips.pdf. (Accessed 13.08.2018).

[12] Analog Devices Inc. Hmc869lc5. http://www.analog.com/media/en/technical-documentation/data-sheets/hmc869.pdf. (Accessed 13.08.2018).

[13] Analog Devices Inc. Hmc626alp5e. http://www.analog.com/media/en/technical-documentation/data-sheets/hmc626a.pdf. (Accessed 13.08.2018).

[14] Analog Devices Inc. Adl5531. http://www.analog.com/media/en/technical-documentation/data-sheets/ADL5531.pdf. (Accessed 13.08.2018).

[15] Y. I. Kim, R. Ainsworth, A. Aryshev, S. T. Boogert, G. Boorman, J. Frisch, A. Heo, Y. Honda, W. H. Hwang, J. Y. Huang, E.-S. Kim, S. H. Kim, A. Lyapin, T. Naito, J. May, D. McCormick, R. E. Mellor, S. Molloy, J. Nelson, S. J. Park, Y. J. Park, M. Ross, S. Shin, C. Swinson, T. Smith, N. Terunuma, T. Tauchi, J. Urakawa, and G.R. White. Cavity beam position monitor system for the accelerator test facility 2. 2013.